

EFFECT OF VARIOUS PARAMETERS ON THE PERFORMANCE OF SALINITY GRADIENT SOLAR POND

*A Thesis Submitted
in Partial Fulfilment of the Requirements
for the Degree of
MASTER OF TECHNOLOGY*

by
YOGESH KUMAR GUPTA

to the
DEPARTMENT OF MECHANICAL ENGINEERING
INDIAN INSTITUTE OF TECHNOLOGY KANPUR
JULY, 1991

ME-1991-M-GUP-EFF

112221

112221

112221

7h
631-44
G959-e

CERTIFICATE

Certified that the thesis entitled 'EFFECT OF VARIOUS PARAMETERS ON THE PERFORMANCE OF SALINITY GRADIENT SOLAR POND' by Mr. Yogesh Kumar Gupta has been carried out under my supervision and that this work has not been submitted elsewhere for the award of a degree.

JULY, 1991


15/7/91
Dr. P.N. Kaul
Assistant Professor
Department of Mech. Engineering
Indian Institute of Technology
Kanpur-208016

ACKNOWLEDGEMENTS

I wish to express my deep sense of gratitude and sincere regards to Dr. P.N. Kaul for his invaluable guidance and constant encouragement in the successful completion of this work.

I am grateful to Drs. Keshav Kant and Manohar Prasad for their timely help and encouragement during my stay at I.I.T. Kanpur.

My sincere thanks are due to M/s. S.P. Singh, G.M., A.T.P.P., Anpara; Rajni Kant, C.E., U.P.S.E.B. and O.P. Vaishya, Ex. En. A.T.P., Anpara, for their help in providing leave to complete my M.Tech.

I express my appreciation and indebtedness to my friends M/s Sandeep Kumar, Sandeep Rastogi, AKM Mohiuddin, S.K. Sinha, Anirudh Gupta, Alok Mishra, Abhilash Chaturvedi and other who apart from making my stay at Kanpur very pleasant and memorable also helped me from time to time.

My thanks are also due to Mr. R.C. Vishwakarma for his excellent typing.

Last but not the least I am grateful to my family members specially my wife Neelima who stood by me through the thick and thin of this assignment.

Yogesh Kumar Gupta

CONTENTS

	<u>PAGE</u>
CERTIFICATE	i
ACKNOWLEDGEMENTS	ii
LIST OF CONTENTS	iii
LIST OF FIGURES	vi
NOMENCLATURE	viii
ABSTRACT	xi
CHAPTER 1 INTRODUCTION	1
1.1 Energy: Crisis and Renewable Sources	1
1.2 Solar Energy	2
1.3 Concept Behind a Solar Pond	4
1.4 What is a Solar Pond ?	4
1.5 Classification of Solar Ponds	6
1.6 Solar Pond Applications	15
CHAPTER 2 REVIEW OF LITERATURE	17
2.1 Conspectus	17
2.2 Analytical Approaches	19
2.3 The First Experimental Pond	24
2.4 Present Work	25

	<u>PAGE</u>
CHAPTER 3 THE MATHEMATICAL FORMULATION	27
3.1 Development of the Model	27
3.2 Attenuation of Solar Radiation in Solar Ponds	28
3.3 Energy Fluxes Within and at the Boundaries of Solar Ponds	30
3.3.1 Energy Balance of the UCZ	31
3.3.2 Energy Balance of the NCZ	34
3.3.3 Energy Balance of the LCZ	37
3.3.4 Energy Balance of the Ground Layers	38
3.4 Boundary Conditions	40
3.5 Numerical Modelling	43
3.6 The Computer Program	46
CHAPTER 4 RESULTS AND DISCUSSIONS	49
4.1 Effect of Transmission Coefficients	49
4.2 Effect of Evaporation Loss	53
4.3 Effect of One Month of Consecutive Cloudy Days	55
4.4 Effect of Water Quality on the Solar Pond Performance	57

LIST OF FIGURES

<u>FIGURE</u>	<u>TITLE</u>	<u>PAGE</u>
1.1	Average solar radiation for ESCAP countries	3
1.2	Schematic representation of a salinity gradient solar pond	10
3.1	Energy fluxes in a solar pond	32
3.2	Energy flux in UCZ	35
3.3	Energy flux in NCZ	35
3.4	Energy flux in LCZ	39
3.5	Energy flux in the ground layer	39
4.1 (a)	Variation of τ for the first six months of the year	50
4.1 (b)	Variation of τ for the whole year	51
4.2	Effect of τ on LCZ temperature	52
4.3	Effect of evaporation loss on LCZ temperature	54
4.4	Effect of one month of consecutive cloudy days on solar pond performance	56
4.5	Effect of water quality on LCZ temperature	58

	<u>PAGE</u>
4.6 LCZ temperature with the load applied on the 60th day and load removed on the 365th day	61
4.7 LCZ temperature with the load applied on the 180th day & load removed on the 365th day	62
4.8 LCZ temperature with the load applied on 180th day, removed on 300th day	63
4.9 LCZ temperature with the load applied on 240th day, removed on 365th day	64
4.10 LCZ temperature with the load applied on 240th day, removed on 300th day	65

NOMENCLATURE

C	Specific heat of water, K/kg K
C_s	Humid heat capacity of air, J/kg K
F_s	Shape factor
h_1	Fraction of radiation reaching depth l_1
h_2	Fraction of radiation reaching depth l_2
h_x	Fraction of radiation reaching depth x
H_a	Annual average solar radiation, W/m ²
H_s	Solar radiation incident on a surface, W/m ²
h_c	Convective heat transfer coefficient, W/m ² K
i	Angle of incidence, deg
K	Thermal conductivity of salt water, W/m K
K_g	Thermal conductivity of ground, W/m K
l_1	UCZ thickness, m
l_2	Depth of NCZ - LCZ interface from the pond surface, m
l_3	Pond depth, m
LCZ	Lower convective zone
NCZ	Non-convective zone

P_s	Vapour pressure of water at the pond surface temperature, mm Hg
P_a	Partial pressure of water vapour in the atmospheric air, mm Hg
P_t	Atmospheric pressure, mm Hg
Q_1, q_1	Heat conduction from LCZ to NCZ, W and W/m^2 respectively
Q_2, q_2	Heat conduction from NCZ to UCZ, W and W/m^2 respectively
Q_c, q_c	Convective heat loss from pond surface, W and W/m^2 respectively
Q_e, q_e	Heat extraction, W and W/m^2 respectively
$Q_{\text{Evap}}, q_{\text{evap}}$	Evaporative heat loss, W and W/m^2 respectively
Q_g, q_g	Heat conduction from LCZ to ground, W and W/m^2 respectively
Q_i, q_i	Incident solar energy, W & W/m^2 respectively
Q_r, q_r	Radiation heat loss, W & W/m^2 respectively
RH	Relative humidity
r	Angle of refraction, deg
t	Time, s
T	Temperature, K

T_a	Ambient temperature, K
T_L	LCZ temperature, K
T_{sky}	Sky temperature, K
T_x	NCZ sublayer temperature, K
T_u	UCZ temperature, K
UCZ	Upper convective zone
W_{qf}	Water quality factor
x	Depth from the pond surface, m
α	Thermal diffusivity, m^2/s
Σ	Emissivity of water
ρ	Density, kg/m^3
σ	Boltzmann constant, $\text{W}/\text{m}^2 \text{ K}^4$
Δ	Angle of declination, deg
ϕ	Latitude, deg
W	Hour angle, deg
λ	Latent heat of vaporization of water, J/kg
τ	Transmission coefficient

ABSTRACT

An algorithm has been developed to predict the thermal behaviour of a salt gradient solar pond. The developed model incorporates a detailed representation of the losses from the surface and the bottom of the pond and uses hourly metrological data for Delhi to predict the pond performance. The effects of water clarity, consecutive days of cloudiness, evaporation loss and different rates of heat removal on a solar pond's performance have also been studied. Validity of assuming a constant transmission coefficient for a solar pond throughout the year has also been verified. It is concluded that though water clarity greatly affects the overall performance of a solar pond, variable transmission coefficients have very little influence on it. The evaporation loss from the surface of a solar pond, which is quite significant during the months of May, June & July every year, does not allow high LCZ temperatures to be reached. Study of several consecutive cloudy days shows that solar pond still offers a relatively reliable solar collector-cum-storage system.

CHAPTER 1

INTRODUCTION

1.1 ENERGY: CRISIS AND RENEWABLE SOURCES

It is well known that energy represents the source of activities of human beings and nature. It was the discovery of new sources of energy like coal, petroleum products and hydroelectricity which provided a tremendous impetus to the industrialisation and it was the quantitative availability of these energy resources which mainly contributed to the pace of development of the, now, industrialised nations. But, unfortunately, the pattern of consumption in the first half of this century has been, rather, wasteful as no attempt seems to have been made to conserve energy with a foresight into the future.

The oil embargo of the early seventies shifted the focus to the renewable sources of energy. There is hardly any disagreement on the importance of harnessing renewable sources of energy, especially solar energy in the immediate future. At a time when world is becoming more and more, aware of the problems of increased pollution and mounting cost, this clean source of energy deserves a serious attention in the world energy plans.

1.2 SOLAR ENERGY

Sun [1,2] the source of solar energy, is a sphere of intensely hot gaseous matter. The rate of energy generation, due to fusion reactions, on the sun is around 12×10^{12} Q ($1Q = 10^{21}$ Joules). Out of this only a very small portion, around 5300 Q enters the earth's atmosphere. Even this small fraction is very huge compared to the total world energy consumption of 0.3 Q per annum. However all this energy that enters the atmosphere, does not reach the surface of the earth. While at a point just outside the atmosphere, the energy intensity is 1353 W/m^2 , the average amount received on the earth is just about 690 W/m^2 . This value may vary with locations, seasons i.e., the day of the year, and the time of the day.

It is observed that the sites lying between latitude of 30°N and 30°S have sufficiently high solar intensities even during winter. India, with its extreme latitude of 8°N and 32°N is fortunately very well placed for solar energy utilization. Actual solar radiation measurement in various ESCAP (Economic and Social Commission for Asia and the Pacific) countries have been used to produce charts of total solar radiation per unit area on unit reception basis. The attached chart of Fig. (1.1) shows that India receives the maximum solar radiation. Average reception for India works out to be 2100 kWh per year per square meter area.

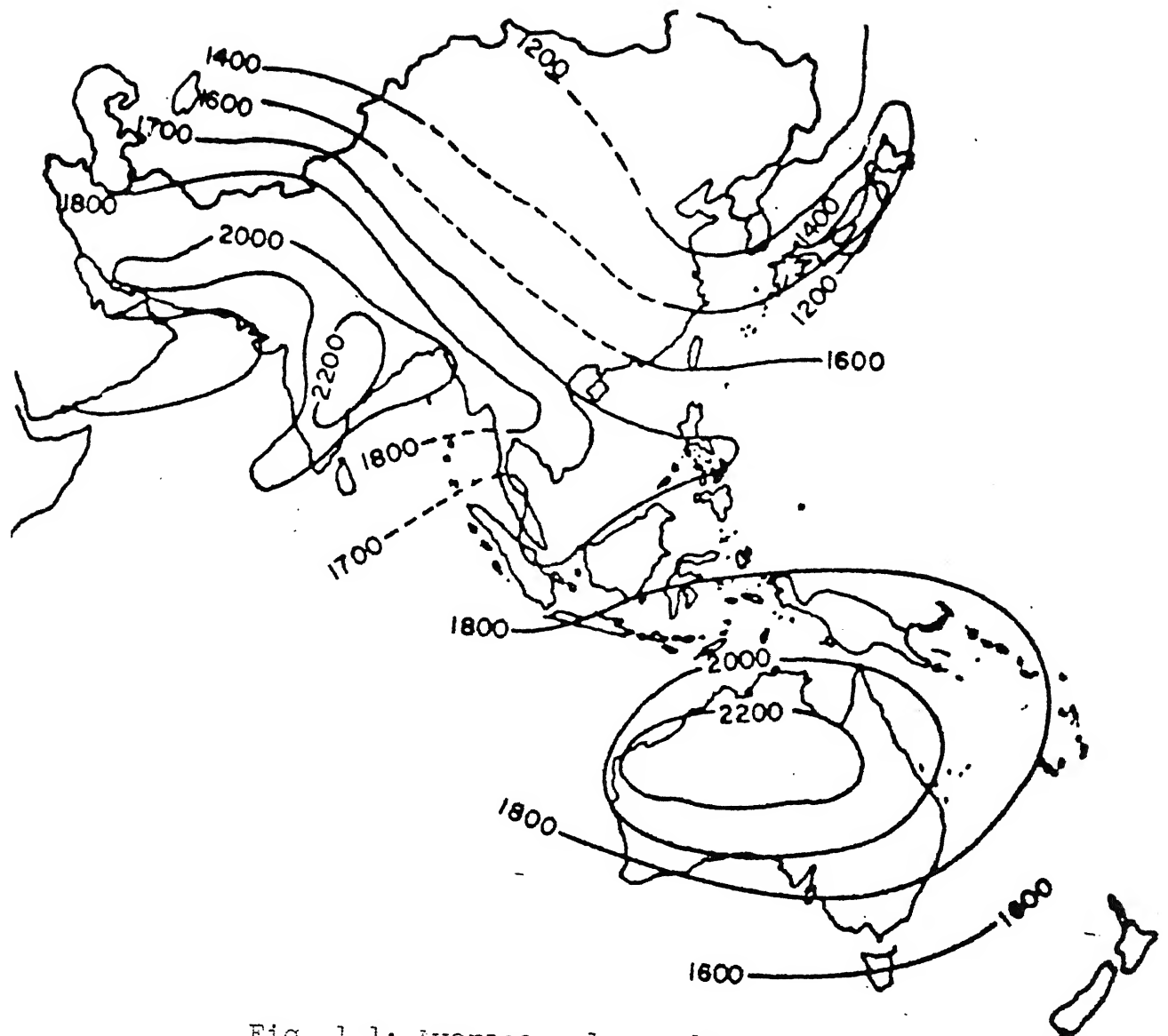


Fig. 1.1: Average solar radiation for ESCAP countries

Main problems being faced by the solar energy utilization programme are its low intensities thereby requiring large collector areas, low overall system efficiencies, and the need of auxiliary equipments due to its intermittent availability.

1.3 CONCEPT BEHIND A SOLAR POND

The separation of the collecting and storage units in the conventional solar system permits the efficient design for each unit. Although the efficiency of such systems is quite high so is the unit cost. These systems can not be scaled up for long term, large energy storage. The large collecting areas and large storage units will be prohibitively expensive. The long term energy storage calls for a different approach. For solar energy to be competitive, the system must be designed where large collecting areas or large storage capacity or both should be cheaply available. Solar pond is one of the concepts where both large collecting areas and storage capacity are inexpensive.

1.4 WHAT IS A SOLAR POND ?

Solar ponds [3,4] are proven, viable, large area collectors of solar energy. These innovative systems collect and store solar energy simultaneously. In a water tank with a black bottom, solar insulations are absorbed at the bottom and

the water in contact is heated up. Heat is transferred from lower layers to upper layers by convection of hot water which being lighter than the cold water, shifts to the top. Energy is lost to the ambient by the hot upper layer, unless means are devised to stop this, most of the energy will be wasted. Thus to store energy, either glazing should be used or convection must be stopped, i.e., ways must be devised to stop this upward movement of water.

The unique characteristic of salinity gradient pond is that, for a large part of their depth, they are non-convective. It is just this stability against transfer of heat by thermal convection that make possible effective collection and storage of solar energy. Stability against convection in salinity gradient ponds is the result of a downward increase of salt concentration, from close to zero at the surface to typically 20-25% near the bottom. The variation in salinity makes the water denser at the bottom even when it is heated to a relatively high temperature by the transmitted solar radiation. Being denser, it remains at the bottom and so its heat is not lost by convection into the surface layer and ultimately to the atmosphere. Salinity variation inside the pond has little effect upon either the solar energy collection or the storage but it stabilizes the pond against convection and thus against heat loss produced by convection in ordinary ponds and lakes.

Given this stability, the only natural process by which heat can be transferred upward from the bottom of a salinity gradient pond is heat conduction, water being opaque to low temperature radiations. Non-convective water thus serves as a partially transparent thermal insulator. One meter of non-convective water has about the same insulating value as six cms of foam, or about five times the insulating value of double glass as commonly used for window and solar energy collectors.

The fact that water is not entirely transparent to solar radiation has important consequences for the pond performance. The infrared and red components of the spectrum are absorbed near the surface and a little over one third of the incident solar energy penetrates to a depth of one meter in clean water (fresh or saline). This fact limits the collection efficiency of solar ponds. However, as compared with glass insulated solar collectors, they have the compensating advantage that there is no minimum threshold radiation level for collection and they collect the same fraction of the incident energy however low the solar input may be.

1.5 CLASSIFICATION OF SOLAR PONDS

The word solar pond in its generalised sense is used to mean a system where water is contained in a man made pond or natural cavity inside earth. The water simultaneously collects and stores energy. The water does not flow past an

absorbing surface as is the case of conventional water heaters. Solar ponds are classified as follows [5].

(1) SHALLOW SOLAR POND (SSP)

It is a large water tank containing water about 5-10 cm in depth. It has a black bottom and a glazing at the top to reduce convective losses. The glazing is in touch with the water. The sides of the tank are well insulated. Most of the solar insulation is absorbed by the blackened bottom and only very little by the successive layers of water. The water is heated by convection. The pond is filled in the morning by cold water and the hot water is drained out in the evening. The hot water is either used or stored in a well insulated tank and is returned to the pond next morning to collect more energy. SSP provides hot water in the range of 40 to 60 °C. There is no long term energy storage, it can at best provide short term storage.

In some of the designs, the water is filled into a plastic bag which rests on a well insulated black surface.

(2) SALT GRADIENT SOLAR PONDS (SGSP) OR NON-CONVECTIVE SOLAR PONDS OR SOLAR PONDS (SP)

This is the concept usually known as the solar ponds. Here water is contained in a big open tank, artificial

or natural, 2 to 3 m deep. The water contains salt, mostly NaCl or Mg Cl₂ such that the concentration of the dissolved salt increases with depth. The solar insolation is absorbed by water at different layers but mostly by the dark coloured bottom of the ponds. A critical value of the salt density gradient is needed to off-set the thermal density gradient set up by the hot water in the bottom layers. Once the concentration of dissolved salt is greater than the critical value, convection will stop and the hot water stays at the bottom. The only mode of transmission of heat to upper layers is conduction, which is a much slower process. The water thus acts as insulation and heat remains trapped in the bottom layers. Under good operating conditions, the storage layers can reach a temperature close to the boiling point of the fluid and at the same time surface layer remains at the ambient temperature. This concept of solar ponds provides an exceptionally large area of collection of the order of square kilometers at an average annual efficiency of 20%. The present collector type of solar water heater has an efficiency of 50%. The difference lies in the order of magnitude of collecting area and cost.

This kind of solar pond is also known as the non-convective solar pond, because of the formation of a non-convective zone. A solar pond essentially consists of three zones as shown in Fig. (1.2). A relatively thin zone (UCZ-Upper Convective Zone) or surface zone at the top, which contains very little amount of salt. The convection is introduced in this zone mainly due to wind contact at the surface. The second zone, which is the most important part of solar pond, is the non-convective zone (NCZ-Non-Convective Zone) or gradient zone. As the name implies, there is no convection in this zone. NCZ transfers heat only by conduction. The third zone is at the bottom which is convective and homogeneous (LCZ-Lower Convective Zone). This zone stores energy. LCZ is present due to the necessity of maintaining NCZ. Suppose the whole pond is non-convective. On a warm sunny day, the temperature at the bottom of the pond will be sufficiently high. The salt layers in contact with the bottom will be heated to the extent that their density is lower than the layers just above them. The bottom layers will therefore move upward. As a result convection starts but remains confined to a certain thickness only. It does not spread upward because above a certain thickness, the negative gradient setup by the thermal currents will be off-set

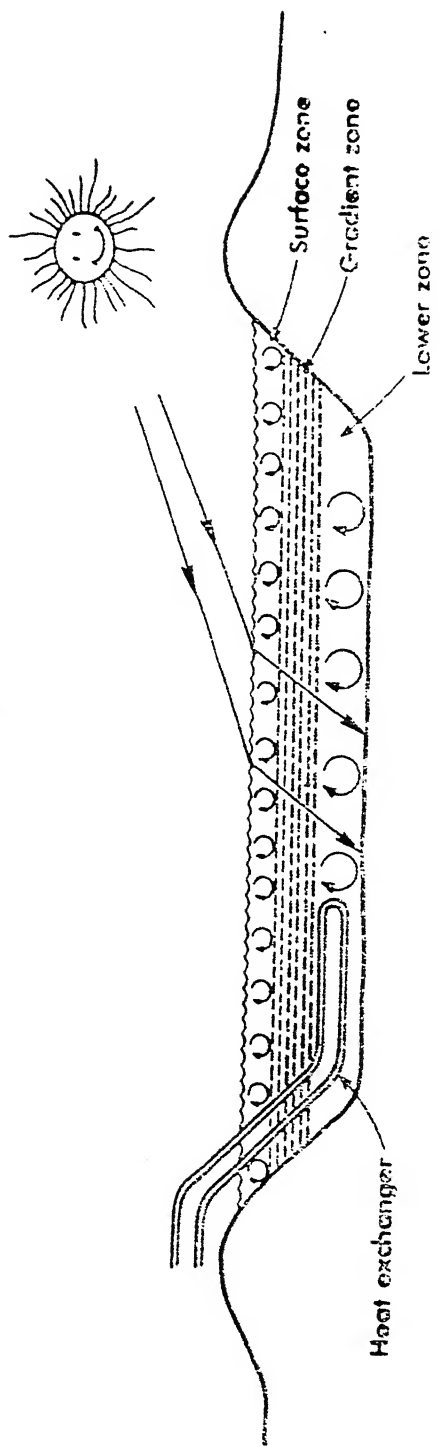


Fig. 1.2: Schematic representation of a salinity gradient solar pond

by the positive gradient of the dissolved salt density or concentration. Thus the magnitude of LCZ depends upon the amount of insolation reaching the bottom. Of course, the formation of LCZ can be prevented by increasing the salt gradient, but this will be uneconomical as large quantity of salt will be required. LCZ is also necessary for heat extraction purposes. UCZ is the principal source of heat loss to the surroundings in a solar pond and the convection in this zone is mainly due to atmospheric wind. Since most of heat is lost from this zone, it is suggested to insulate the ponds against this loss by spreading transparent plastic covers over the pond surface.

The zone boundaries, in general, are not stationary in time. These move, either decreasing or increasing the zone thickness. This motion is usually very slow, typically of the order of a few cms per month. The boundaries move so as to increase the NCZ thickness (or decrease the LCZ thickness) when the temperature gradient is low and vice versa i.e...decrease in the NCZ thickness (or increase in LCZ thickness) when the temperature gradient is high.

This is the solar pond which has been studied in some depth in this thesis.

(3) PARTITIONED SOLAR PONDS (PSP)

In salt gradient ponds it is proposed to separate out LCZ from NCZ by placing a horizontal transparent plastic membrane at an appropriate depth. The requirement of the salt will be much less because maximum salt is required in the LCZ which is PSP will have pure water. It is hoped that PSP will be more stable during energy extraction. NCZ will not be disturbed during fluid removal and injection. A fast rate of energy extraction is possible. Insertion of more than one partition is also proposed. Another partition is advocated to separate NCZ and UCZ. PSP appears to be attractive but larger collection areas are not feasible with it.

(4) VISCOSITY STABILIZED PONDS

Convection can be suppressed if the viscosity of the water can be increased to such an extent that movement of water is not possible. This can be done by adding certain gelling and thickening agents to the water. The pond contents are now semi-solids. Materials suitable for viscosity stabilised ponds should have high transmittance for solar radiation, high thickening efficiency and should be able to perform at temperatures upto 60°C. It is certain that the

proposal will not be economically competitive with salt gradient ponds. Carboxy-vinyl polymer and cellulose derivatives have been found useful as thickening agents.

(5) MEMBRANE STRATIFIED SOLAR POND (MSSP)

In flat-plate solar collector, honey comb structure is used to suppress convection. Similar principle has been proposed in MSSP. The convection in the upper layers is suppressed by placing a suitable number of vertical membrane or horizontal sheets or vertical tubes [6]. The pond now has only two zones LCZ and NCZ. In MSSP no salt is needed anywhere making the concept economically attractive.

Maintaining the salt gradient in a SGSP usually requires vigilance, and in many locations salt contamination is potentially a large environmental hazard due to persistence of positive ions in soils. In addition to the toxicity to vegetation caused by overly salty soils, a major danger of salt pollution involves the detrimental effect of salt in drinking water upon people susceptible to hypertension and other salt related diseases. This concept will be more efficient than SGSP due to the absence of UCZ which loses a lot of heat to the surroundings. MSSP

membrances can be placed very close to the surface, almost completely eliminating the UCZ to the surroundings. Three kinds of membranes suggested are; horizontal sheet, vertical tube and vertical sheet. Teflon is suggested to be the suitable membrane material because of its long life, high transparency, inert nature virtually to all chemicals, commercial availability in all sizes and thicknesses. Water is the most preferred liquid but others like ethanol, combination of water and ethanol can also be used.

(6) SATURATED SOLAR PONDS

In this concept, the salt density gradient is maintained by the temperature gradient. A salt is chosen for which solubility is a function of temperature. The pond water is kept saturated with such a salt at all levels and since the pond is hotter at the bottom than the top, more salt is dissolved in the bottom than the top. As there is no vertical diffusion of the salt, SSP requires no maintenance. $Mg Cl_2$ is the most preferred salt for this kind of concept, Borax and KNO_3 are other salts. Such ponds have been built on small laboratory scales only. The possible precipitation at the bottom of the pond of white salt crystals of $MgCl_2$ will reflect more solar radiation rather than absorbing it.

1.6 SOLAR POND APPLICATIONS

Solar ponds collect and store energy for use at temperatures below the boiling point of the lower zone brine. They are lower in cost than the conventional flat plate collectors in almost all locations and much lower in favourable locations. Typically averaged energy gain per unit area of pond is comparable to that of a flat plate collector for the same average values of solar input and output temperature and the pond advantages are to be found in the lower cost and the large intrinsic heat storage capacity. Pond limitations are the impossibility of mounting on roofs and the heat losses to the earth that make uninsulated small ponds inefficient. On account of these losses, ponds of only a few hundred square meters area for individual house or water heating are not economically competitive.

Within these limitations, solar ponds have a wide range of potential application for providing low temperature heat at a low cost. Following are some of the areas where solar ponds have been used advantageously.

- (a) Power production
- (b) Space heating

- (c) Crop drying
- (d) Domestic water or swimming pool heating
- (e) Desalination
- (f) Industrial process heat

CHAPTER 2

REVIEW OF LITERATURE

2.1 CONSPECTUS

Unlike other thermal collectors, the salinity gradient solar pond is a natural phenomenon. It is found in a few places in the world where a rare combination of circumstances results in a body of water more saline at some depth below the surface than it is at the surface. The first study of natural solar heated salinity-gradient lakes was that published by Kalecsinsky [7]. He collected temperature and salinity data from several lakes in Transylvania (Hungary) and demonstrated by analysis and laboratory experiments that the heating, to temperature as high as 70°C, was caused by solar energy penetration into water that was maintained non-convective by the density gradient resulting from dissolved salt. It is interesting that even at that time Kalecsinsky proposed the use of artificial solar pond to collect and store solar energy for domestic and industrial applications.

Following Kalecsinsky's work there was some continuing study of the natural solar heated lakes in Transylvania, but there was no immediate attempt to act on the proposal to construct a solar pond for practical utilization of solar energy.

The SGSP was again proposed as a device for collecting and storing solar energy in 1948 by R. Bloch in Israel and solar pond research was begun there ten years later by Tabor. Bloch conceived the use of SGSP on the basis of the heating observed in the Transylvania lakes, first studied by Kalecsinsky. This first period of solar pond research in Israel continued until 1966 and resulted in very important contribution to our understanding of the problems involved in operating solar ponds and in developing their possible applications. The primary goal was power production, but some studies were made of other possible applications by Tabor and Matz [8].

Solar ponds were studied subsequently in Australia by Davey (1968) [9], in Chile by Hirschmann (1970) [10], in India by Jain (1973) [11], and in the USSR by Usmanov (1971) & Eliseev (1973) [12]. The Australian pond, which was operated for two years, constituted a preliminary feasibility demonstration. Hirschmann explored the possibility of using ponds for electric power generation, process heat, and desalination of water. The work in the USSR consisted of theoretical studies and small laboratory experiments. None of these early works outside of Israel were continued for more than a few years.

The present period of pond research began in 1974, with a theoretical study of ponds for space heating carried out by

Rabl and Nielsen (1975) [13], small pond experiments in Canada by Saulnier et al (1975), [14], possible application of solar ponds to house as well as food and paper process heating by Styris et.al [15], a scheme for modifying the dead sea into a huge solar pond by Assaf [16], the performance of the ground storage beneath a solar pond by Akbarzadeh and Ahmadi [17]. Pond work has been continuous in several sites since that time and there is now activity in many countries.

2.2 ANALYTICAL APPROACHES

There have been a number of efforts to solve the heat and mass diffusion equations, applied to solar ponds, analytically and predict their performance. A few important contributions in this direction are discussed below.

2.2.1 WEINBERGER'S APPROACH

Weinberger [18] was the first to study the physics of the problem. He developed expressions for the absorption of solar radiation, temperature rise, rate of energy withdrawl, efficiency and stability conditions of the solar pond. In his analysis Weinberger made use of the following assumptions:

- (1) The pond is of infinite size; edge losses are negligible and one dimensional conduction holds.
- (2) Thermal properties of salt water and ground are the same and constant.

- (3) Natural thermal convection is prevented due to high salt gradient.
- (4) No distinction is made between direct and diffuse radiation.
- (5) Effect of cloudiness is neglected and
- (6) Salt solution remains transparent even after long exposures.

Based on the above assumptions, the temperature distribution $T(x, t)$ in the pond containing internal source of heat $H(x, t)$ is governed by the following diffusion equation

$$\frac{\partial}{\partial x} (K \frac{\partial T}{\partial x}) = \rho C \left(\frac{\partial T}{\partial t} \right) - H(x, t)$$

Weinberger assumed K , ρ and C to be constant, hence

$$\frac{\partial^2 T}{\partial x^2} = \frac{1}{\alpha} \frac{\partial T}{\partial t} - \frac{H(x, t)}{K}$$

Where,

$$\alpha = \frac{K}{\rho C} \quad (\text{Thermal diffusivity})$$

Weinberger integrated the above equation for the following five boundary conditions to predict the temperature profile $T(x, t)$ of the pond:

- (1) The solar flux $\phi(x, t)$ that reaches the bottom is completely absorbed there.

(2) $H(x,t) = - \left[\frac{\partial \phi}{\partial x} \right]_{(x,t)}$ is the solar energy absorbed at a depth x in the water body.

(3) Energy is removed at a rate $U(t)$ from the bottom of the pond.

(4) The temperature of the pond surface is equal to the ambient temperature.

(5) The initial temperature of the pond is known.

2.2.2 RABL AND NIELSEN'S MODEL

Ari Rabl and Carl E. Nielsen [13] made assumptions that were very similar to those of Weinberger but were more realistic in nature to the problems of solar ponds. They considered the presence of a convective zone in the pond and also took different thermal properties for the ground and the salt water. They thus altered the assumption numbers (2) and (3) of the Weinberger approach. They also restricted their attention to the steady state condition because solar ponds are primarily meant for long term energy storage. Their analysis can be broadly divided into four steps:

(1) Calculation of time independent component of temperature

For this they solved the steady state heat conduction equation and the applied energy balance equation to the insulating layer (NCZ).

(2) Calculation of the Sinusoidally varying component of temperature:

This requires the heat balance equation of the convective zone to include the heat exchange from the ground as well as the heating and cooling of water in the convective zone.

(3) Approach to steady state:

They considered two different cases; (a) slab of finite thickness and (b) the semi-infinite solid. They assumed zero temperature throughout the ground and the surface temperature of the UC layer to be constant, and equal to the ambient temperature.

(4) Estimation of edge losses in a finite pond:

The pond was assumed to be circular with radius 'a' and depth 't'. The thermal properties of the ground and salt water were assumed to be constant. Presence of convective zone and time variation were neglected. All radiations were assumed to be absorbed at the bottom of the pond.

2.2.3 KOOI'S APPROACH

C.F. Kooi [19] analysed the thermal behaviour of a solar pond treating it as a steady state flat plate collector. According to this model, a solar pond has three zones:

- (1) UCZ (Upper Convective Zone) having low and uniform salt content and a constant temperature close to the ambient temperature.
- (2) UCZ followed by NCZ (Non-Convective Zone) in which the salt content increases with depth.
- (3) NCZ followed by LCZ (Lower Convective Zone).

Here salt content and temperature are nearly constant Kooi, however, does not consider the edge and the bottom losses in his analysis.

2.3.4 HAWALDER AND BRINKWORTH APPROACH

Hawalder and Brinkworth [20] studied the effect of:

- (1) Extinction coefficient of solar radiation
- (2) Thickness of storage zone
- (3) Bottom insulation
- (4) Load application on the performance of a solar pond.

They combined the surface heat loss by convection, radiation and evaporation into a single term as:

$$Q_{LS} = U_{LS} (\theta_s - \theta_a)$$

Where Q_{LS} Surface heat loss

U_{LS} Surface heat loss coefficient

θ_s Surface temperature

θ_a Ambient temperature

For determining U_{LS} they used empirical equations obtained from the measurement of losses from a body of convecting fluid at a nearly uniform temperature above the ambient.

2.3 FIRST EXPERIMENTAL POND

The first experimental pond was constructed by Prof Tabor [21] in 1958 in Israel. The results obtained, however, were not encouraging. This was attributed to low solubility of the common salt used. The following aspects were studied in detail:

1. Amount of solar radiation reaching the bottom of the pond.
2. Conditions for stability.
3. Rate of diffusion of salt.
4. Extraction of heat from the lower layer.
5. Effect of wind induced waves.
6. Effect of evaporation and
7. Effect of dirt and dust falling on the pond.

Based on the experiences gained during the project the following were suggested as the major problems to be tackled, to make the use of solar ponds economical:

1. Extracting heat from the bottom without disturbing the density gradient.

2. Suppression of upper zone mixing due to wind.
3. Method of keeping the pond clear.
4. Suppression of biological growth in the pond with time.

2.4 PRESENT WORK

In this work a computer model of a large solar pond to be located in the northern part of India has been developed. The input to the program are the hourly solar radiation, ambient temperature and relative humidity data for New Delhi. Also informations about the depth of pond, initial temperature of pond, thermal properties of salt water and ground are provided. The temperature rise of the storage zone of the pond for various rates of energy removal is the output from the program. Basic one dimensional heat transfer equations are developed incorporating the individual terms for ground loss, and convection, radiation and evaporation heat loss from the pond surface. These are then solved numerically with appropriate initial and boundary conditions. An improved equation for transmission of solar radiation as suggested by P.T. Tsilingris has been used. The effect of the clarity of pond's water is taken into account with the introduction of

a water quality factor. Pond's performance under various rates of heat removal, different load application and removal time schedules, variable and constant transmission co-efficients and consecutive cloudy days is analysed and discussed.

CHAPTER 3

THE MATHEMATICAL FORMULATION

The salt gradient solar pond, considered in the present work, consists of three distinct zones: an upper convective zone (UCZ), a non-convective concentration gradient zone (NCZ), and a lower convective zone (LCZ) or energy storage zone. The thermal performance of such a pond depends on the thickness of each of the above three zones.

3.1 DEVELOPMENT OF THE MODEL

The pond is considered to be one dimensional with respect to heat transfer, with constant depth and of infinite area. The effect of side boundaries and edges of the pond is ignored. This assumption may not cause significant error in simulation results because for practical purposes pond's lateral dimensions are very large with respect to its depth. The model considers the transmission of the incident solar radiation through the surface, its attenuation as it passes the subsequent water layers and the final absorption in the LCZ. The bottom of the pond is assumed to be perfectly absorbing and the radiation entering the LCZ is completely absorbed there, either in the water body or at the bottom. It is further assumed that the stability of the pond maintained even at high LCZ temperatures.

The temperature of the LCZ being higher than that of other layers, it loses heat to ground and NCZ. The UCZ loses heat to environment by convection, radiation and evaporation.

In a subsequent paragraph the above mentioned processes are discussed in full detail and presented in a mathematical form, using basic principles of heat transfer.

3.2 ATTENUATION OF SOLAR RADIATION IN A SOLAR POND

The performance of a solar pond largely depends on the amount of the radiation which reaches the bottom region. The UCZ absorbs a large portion of the long wave solar radiation. This portion of the solar input can not be utilized and is eventually dissipated to the atmosphere.

The most widely known mathematical expression on transmission of solar radiation through a solar pond in literature is the Rabl and Nielsen (R.N.) [13] four term exponential expression given by

$$H(x) = \tau H_s \sum_{i=1}^4 \mu_i \cdot \exp(-n_i x) \quad (3.1)$$

Where μ_i and n_i are empirical coefficients and have different values for different radiation wave length bands. The above expression has been reduced to a simple algebraic equation

$$h(x) = 0.36 - 0.08 \ln x; 10 \text{ m} \geq x \geq 0.01 \text{ m} \quad (3.2)$$

by Bryant and Colbeck [22]. This relation gives the per unit attenuation of solar radiation with depth x of the pond. The expression, however, is not very accurate as it

has been derived from results based on old and early pond data. More recently P.T. Tsilingris [23] has suggested the following expression using numerical techniques and dividing the solar spectrum into 19 non-equally spaced bands

$$h(x) = \sum_{i=1}^{19} \mu_i \exp(-n_i x) \quad (3.3)$$

This expression may be fitted by polynomials with a high accuracy such as the one of fourth degree,

$$\begin{aligned} h(x) = & 0.67031 - 0.35170 x + 0.19785 x^2 \\ & - 0.05567 x^3 + 0.0058 x^4 \end{aligned} \quad (3.4)$$

and this can be further approximated with good accuracy by the simple algebraic relationship

$$h(x) = a - b \ln x, \quad 5.5m \geq x \geq 0.2 m \quad (3.5)$$

Where $a = 0.46$ & $b = 0.0953$

The transmission coefficient can be calculated using Fresnel relations [2], as:

$$\tau = 0.5 \left[\frac{\sin^2(i - r)}{\sin^2(i + r)} + \frac{\tan^2(i - r)}{\tan^2(i + r)} \right] \quad (3.6)$$

Where r and i are computed using the Snell's law i.e.,

$$\frac{\sin i}{\sin r} = 1.33 \quad (3.7)$$

and the incident angle relation, respectively.

$$\cos i = \sin \Delta \sin \phi + \cos \Delta \cos \phi \cos w \quad (3.8)$$

Where,

Δ , the declination angle is given by

$$\Delta = 23.45 \sin \left(2\pi \frac{284 + d}{365} \right), \quad (3.9)$$

d is the day of the year with value of 1 for first January,
and the hour angle

$$W = \frac{\pi}{12} (12 - hr) \quad (3.10)$$

If we introduce a dimensionless water quality factor,
 w_{qf} , [23] which represents for clarity status of the solar pond
water, being assumed as 1 for distilled or ideally clear
natural water, then, eqn. (3.5) can be rewritten as:

$$h(x) = w_{qf} (a - b \ln x) \quad (3.11)$$

Where $w_{qf} = 0.7$ to 0.75 for practically pure pond water.

The amount of radiation reaching depth x of the pond
is then given by

$$H(x) = h(x) \tau H_s \quad (3.12)$$

3.3 ENERGY FLUXES WITHIN AND AT THE BOUNDARIES OF THE POND

Heat energy is lost from a pond primarily by convection,
evaporation and long wave radiation from the surface of the
pond to the sky and by conduction to the earth at the bottom.
Besides, a fraction of the solar radiation falling on the pond
is reflected back and hence is not available to the pond for
utilization.

There is transfer of heat energy due to interaction between the layers of the pond, as they are at different temperatures. The LCZ, owing to its higher temperature conducts heat to NCZ and to the ground. The NCZ, in turn, conducts heat to the UCZ which loses it to the ambient air. These energy fluxes are shown in Fig. 3.1.

In order to simulate the behaviour of the pond, energy balances of the various zones in the pond are considered and the resulting equations solved simultaneously.

3.3.1 ENERGY BALANCE OF THE UCZ

The energy exchanges of the UCZ with ambient air and the NCZ are shown in Fig. 3.2. The UCZ is assumed to be at a uniform temperature T_u . The UCZ receives energy from the sun. Some part of incident energy is reflected back. The fraction of incident energy able to pass the surface layer is dependent on the transmission coefficient.

Hence,

$$\text{Incident radiation energy transmitted} = \tau H_s \quad (3.13a)$$

Radiation energy transmitted through

$$\text{UCZ;} = \tau H_s h_{11} \quad (3.13b)$$

$$\text{Energy conducted from NCZ to UCZ} = K \left. \frac{\partial T}{\partial x} \right|_{x=l_1} \quad (3.14)$$

Energy lost by convection from the surface

$$\text{of the pond, } q_c = h_c (T_u - T_a) \quad (3.15)$$

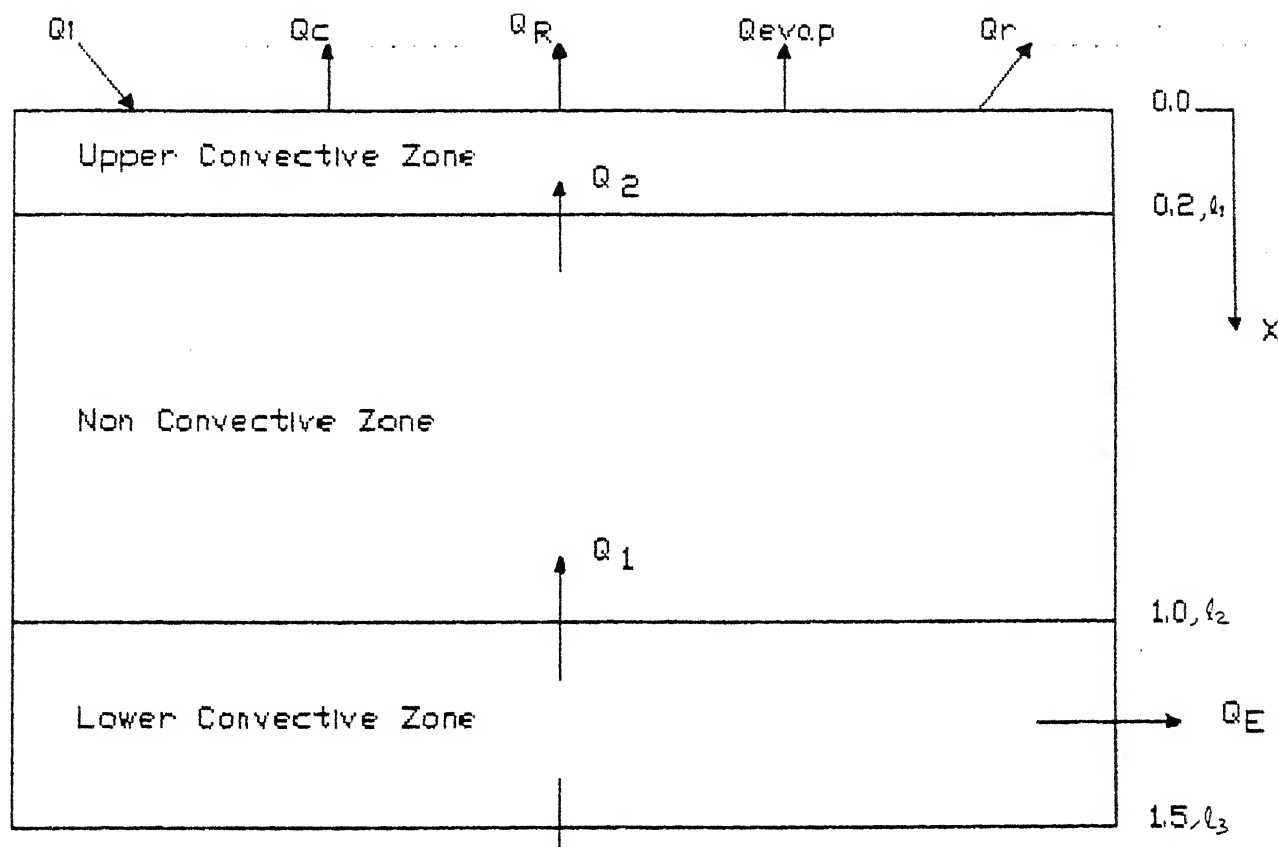


Fig 3.1 Energy Fluxes In Solar Pond

(All Depth Dimensions are in meters)

Where h_c , the wind convective heat transfer coefficient [2], is given by

$$h_c = 5.7 + 3.8 V, \text{ w/m}^2 \text{ K} \quad (3.16)$$

Where V is wind velocity in m/s

$$\text{Energy lost by radiation, } q_R = \epsilon \sigma F_s (T_u^4 - T_{sky}^4) \quad (3.17)$$

Where $T_{sky} = T_a - 6.0$ [24]

$$\text{Energy lost by evaporation [25], } q_{evap} = \frac{\lambda h_c}{1.6 C_s P_t} (P_s - P_a) \quad (3.18)$$

$$\text{Where [26] } P_s = \text{Exp} (18.403 - \frac{3885}{T_u + 230}) , \text{ mm Hg} \quad (3.19)$$

$$\text{and } P_a = \text{RH} \cdot P_s , \text{ mm Hg}$$

Using the above expressions of eqns (3.13) to (3.19), we can write the total inward flux of UCZ as

$$\tau H_s + K \frac{\partial T}{\partial x} \Big|_{x=l_i} \quad (a)$$

and the total outward flux of UCZ as

$$\begin{aligned} h_c (T_u - T_a) + \epsilon \sigma F_s (T_u^4 - T_{sky}^4) + h_{l_i} \tau H_s \\ + \frac{\lambda h_c}{1.6 C_s P_t} (P_s - P_a) \end{aligned} \quad (b)$$

The difference in the expressions a & b is responsible for the heat accumulation in the UCZ and hence its temperature rise. Hence we can write

$$\begin{aligned} l_i \rho C \frac{\partial^2 u}{\partial t^2} = \tau H_s + K \frac{\partial T}{\partial x} \Big|_{x=l_i} - [h_{l_i} \tau H_s + h_c (T_u - T_a) \\ + \epsilon \sigma F_s (T_u^4 - T_{sky}^4) + \frac{\lambda h_c}{1.6 C_s P_t} (P_s - P_a)] \end{aligned} \quad (3.20)$$

by re-arranging and transposing, we get

$$\begin{aligned}
 \frac{\partial T_u}{\partial t} &= \frac{\alpha}{K l_1} \tau_{H_s} (1 - h_{l_1}) + \frac{\alpha}{l_1} \frac{\partial T}{\partial x} \Big|_{x=l_1} \\
 &\quad - \frac{h_c \alpha}{K l_1} (T_u - T_a) - \frac{\alpha \epsilon \sigma F_s (T_u^4 - T_{sky}^4)}{K l_1} \\
 &\quad - \frac{\lambda h_c \alpha (P_s - P_a)}{1.6 C_s P_t K l_1} \tag{3.21}
 \end{aligned}$$

Where $\alpha = \frac{K}{\rho C}$, Thermal diffusivity of salt water (3.22)

3.3.2 ENERGY BALANCE OF NCZ

The NCZ in a solar pond is a very vital portion, as it acts as the insulation and hence reduces the loss of energy from the LCZ. But as the thickness of NCZ increases, the energy flux reaching the LCZ decreases. So for better performance of the pond, the thickness of the NCZ must be optimised for better insulation and lower attenuation. The energy flux terms in a typical NCZ are as shown in Fig. 3.3.

The NCZ being at a higher temperature than the UCZ conducts heat to UCZ. Similarly because of the higher temperature of the LCZ, the NCZ receives energy by conduction from LCZ. NCZ also absorbs a portion of the incoming solar radiation and transmits the rest to the LCZ. For the purpose of analysis NCZ is divided into a number of smaller elements. The above mentioned energy flux terms for a typical element

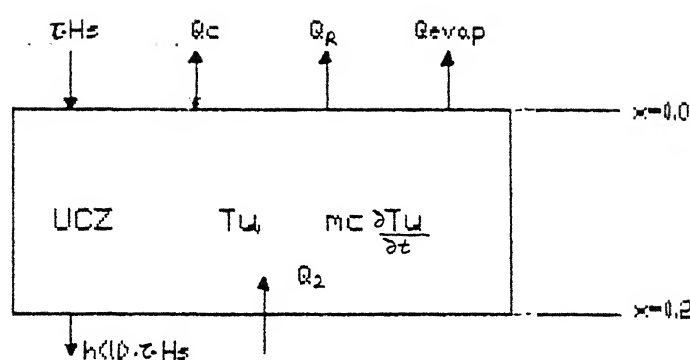


Fig 3.2 Energy flux in UCZ

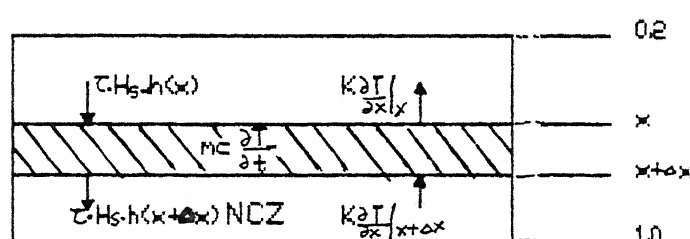


Fig 3.3 Energy flux in NCZ

in the NCZ can be expressed mathematically as:

$$\text{Energy lost to the upper layer} = K \left. \frac{\partial T}{\partial x} \right|_x \quad (3.23)$$

$$\text{Energy gained from the bottom layer} = K \left. \frac{\partial T}{\partial x} \right|_{x+\Delta x}$$

Energy input due to solar radiation, using equation

$$(3.12), H(x) = h_x \tau H_s \quad (3.24)$$

Energy leaving the elements due to transmission of radiation

$$\text{is} = h_{x+\Delta x} \tau H_s \quad (3.25)$$

The difference between the input and the output terms of the elements is responsible for the temperature rise of the element.

Hence,

$$\rho C \Delta x \frac{dT}{dt} = [K \left. \frac{\partial T}{\partial x} \right|_{x+\Delta x} + \tau h_x H_s] - [K \left. \frac{\partial T}{\partial x} \right|_x + \tau h_{x+\Delta x} H_s] \quad (3.26)$$

or

$$\rho C \frac{dT}{dt} = \frac{K \left. \frac{\partial T}{\partial x} \right|_{x+\Delta x} - K \left. \frac{\partial T}{\partial x} \right|_x}{\Delta x} + \tau H_s \left(\frac{h_x - h_{x+\Delta x}}{\Delta x} \right) \quad (3.27)$$

or

$$\rho C \frac{dT}{dt} = K \frac{\partial^2 T}{\partial x^2} + \tau H_s \left(- \frac{dh}{dx} \right) \quad (3.28)$$

But from Eqn. (3.5) $h = a - b \ln x$

hence,

$$\frac{dh}{dx} = -\frac{b}{x} \quad (3.29)$$

Substituting eqn (3.29) in eqn. (3.28), we get

$$\rho C \frac{\partial T}{\partial t} = K \frac{\partial^2 T}{\partial x^2} + \frac{\tau H_s b}{x} \quad (3.30)$$

$$\text{or } \frac{\partial T}{\partial t} = \alpha \frac{\partial^2 T}{\partial x^2} + \frac{\alpha}{K} \frac{\tau H_s b}{x} \quad (3.31)$$

The variation of temperature in the NCZ can then be obtained by solving eqn. (3.31) subject to the boundary conditions applicable to the NCZ.

3.3.3 ENERGY BALANCE OF THE LCZ

The various energy flux terms involved in the LCZ are as shown in Fig. 3.4. Due to presence of convection, this zone is assumed to have a constant temperature T_1 . In mathematical form these interactions of energy fluxes can be written as follows:

$$\text{Energy conducted to the NCZ, } q_1 = K \frac{\partial T}{\partial x} \Big|_{x=l_2} \quad (3.32)$$

$$\text{Energy conducted to the ground, } q_g = K_G \frac{\partial T}{\partial x} \Big|_{x=l_3} \quad (3.33)$$

$$\text{Energy extracted for useful applications} = q_e$$

$$\text{Energy received by the LCZ} = h_{l_2} \tau H_s \quad (3.34)$$

$$\text{Hence, total inward flux} = h_{l_2} \tau H_s \quad (3.35)$$

$$\text{and total outward flux} = K \left. \frac{\partial T}{\partial x} \right|_{x=1_2} + K_G \left. \frac{\partial T_G}{\partial x} \right|_{x=1_3} + q_e \quad (3.36)$$

The difference between expressions (3.35) and (3.36) is responsible for the heat accumulation in the LCZ, hence,

$$(1_3 - 1_2) \rho C \frac{\partial T_L}{\partial t} = h_{1_2} \tau_{H_s} - [K \left. \frac{\partial T}{\partial x} \right|_{x=1_2} + K_G \left. \frac{\partial T_G}{\partial x} \right|_{x=1_3} + q_e] \quad (3.37)$$

By transposing we get,

$$\begin{aligned} \frac{\partial T_L}{\partial t} &= \frac{h_{1_2} \tau_{H_s}}{\rho C (1_3 - 1_2)} - \frac{K}{(1_3 - 1_2) \rho C} \left. \frac{\partial T}{\partial x} \right|_{x=1_2} \\ &\quad - \frac{K_G}{\rho C (1_3 - 1_2)} \left. \frac{\partial T_G}{\partial x} \right|_{x=1_3} - \frac{q_e}{\rho C (1_3 - 1_2)} \end{aligned} \quad (3.38)$$

Eqn. (3.38) can then be solved in conjunction with other equations subject to appropriate boundary conditions to predict the behaviour of the LCZ.

3.3.4 ENERGY BALANCE OF THE GROUND LAYERS

The ground layers receives energy only from the LCZ and conduct it to their lower layers. Since there are temperature variations with depth as well as time, the ground is divided into smaller elements parallel to the lower convective zone where in temperature can be assumed to be uniform with depth without incurring appreciable error. The energy flux terms for such a layer are shown in Fig. 3.5 and can be written mathematically as follows:

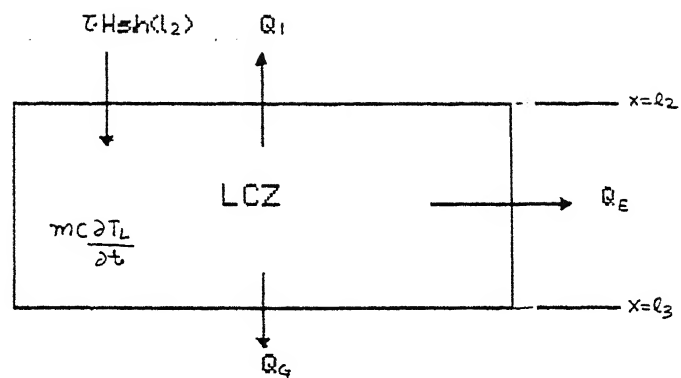


Fig 3.4 Energy flux in LCZ

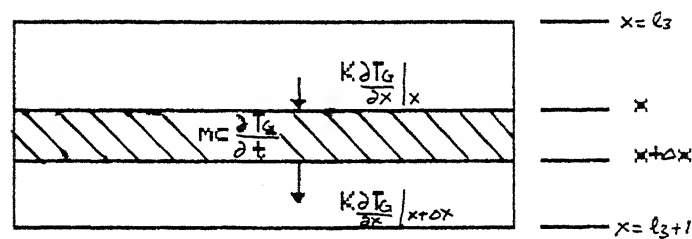


Fig 3.5 Energy flux in ground layer

Energy conducted from the upper ground layer

$$= - K_G \frac{\partial T_G}{\partial x} \Big|_x \quad (3.39)$$

Energy conducted to the lower ground layer

$$= - K_G \frac{\partial T_G}{\partial x} \Big|_{x+\Delta x} \quad (3.40)$$

The difference between (3.39) and (3.40) is then equated to the rate of energy storage

$$\rho C \Delta x \frac{\partial^2 T_G}{\partial t^2} = - K_G \frac{\partial T_G}{\partial x} \Big|_x - (- K_G \frac{\partial T_G}{\partial x} \Big|_{x+\Delta x}) \quad (3.41)$$

or

$$\rho C \Delta x \frac{\partial^2 T_G}{\partial t^2} = K_G \left[\frac{\partial T_G}{\partial x} \Big|_{x+\Delta x} - \frac{\partial T_G}{\partial x} \Big|_x \right] \quad (3.42)$$

By transposing we get,

$$\frac{\partial^2 T_G}{\partial t^2} = \alpha_G \frac{\partial^2 T_G}{\partial x^2} \quad (3.43)$$

Where $\alpha_G = \frac{K_G}{\rho C}$, Thermal diffusivity of the ground

Eqn. (3.43) simulates the temperature variations of the ground layers.

3.4 BOUNDARY CONDITIONS

Temperature distribution in the solar pond is then obtained by solving the following equations simultaneously subject to the boundary conditions listed below.

$$\begin{aligned}
 \frac{\partial T_u}{\partial t} &= \frac{\alpha}{kl_1} \tau_{Hs} (1 - h_{l_1}) + \frac{\alpha}{l_1} \frac{\partial T}{\partial x} \Big|_{x=l_1} \\
 &\quad - \frac{h_c \alpha}{kl_1} (T_u - T_a) - \frac{\alpha \epsilon F_s \sigma (T_u^4 - T_{sky}^4)}{kl_1} \\
 &\quad - \frac{\alpha \lambda h_c (P_s - P_a)}{kl_1 1.6 C_s P_t} \quad (3.21)
 \end{aligned}$$

$$\frac{\partial T}{\partial t} = \alpha \frac{\partial^2 T}{\partial x^2} + \frac{\alpha}{K} \frac{\tau_{Hs} b}{x} \quad (3.31)$$

$$\begin{aligned}
 \frac{\partial T_L}{\partial t} &= \frac{h_{l_2} \tau_{Hs}}{\rho C (l_3 - l_2)} - \frac{K}{(l_3 - l_2) \rho C} \frac{\partial T}{\partial x} \Big|_{x=l_2} \\
 &\quad - \frac{K_G}{\rho C (l_3 - l_2)} \frac{\partial T_G}{\partial x} \Big|_{x=l_3} - \frac{q_e}{\rho C (l_3 - l_2)} \quad (3.38)
 \end{aligned}$$

and

$$\frac{\partial T_G}{\partial t} = \alpha_G \frac{\partial^2 T_G}{\partial x^2} \quad (3.43)$$

(1) The upper convective zone surface temperature is equal to ambient temperature at all times i.e.,

$$T_u = T_a, \quad t \geq 0 \quad (3.44)$$

(2) The temperature of the NCZ at $x = l_1$ is equal to the temperature of the UCZ at all times i.e., there is no abrupt change of temperature at the interface.

This can be written mathematically as:

$$T(x) = T_u \quad \text{at} \quad x = l_1, \quad t \geq 0 \quad (3.45)$$

(3) Temperature of the NCZ at $x = l_2$ is the same as the temperature of the LCZ

$$T(x) = T_L \text{ at } x = l_2, \quad t > 0 \quad (3.46)$$

(4) The bottom of the pond is assumed to be at a temperature equal to that of the LCZ.

$$T_G(x) = T_L \text{ at } x = l_3, \quad t > 0 \quad (3.47)$$

(5) Temperature of the ground below a certain depth from the bottom of the pond (1.0 m in this case) is equal to the ambient temperature.

$$T_{G_0}(x) = T_{G_0} \text{ at } x = 1.5 + 1.0, \quad t > 0 \quad (3.48)$$

(6) The pond is assumed to be at the ambient temperature throughout its depth initially i.e.,

$$\begin{aligned}
 T_u &= T_a \\
 T(x) &= T_a \quad \forall x \\
 T_L &= T_a \\
 T_G(x) &= T_a \quad \forall x
 \end{aligned}
 \quad \text{at } t = 0 \quad (3.49)$$

Thus for the solution of the problem eqns. (3.21), (3.31), (3.38) and (3.43) have to be solved simultaneously subject to the boundary conditions given by eqns. (3.44), (3.45), (3.36), (3.37), (3.38) and (3.49).

3.5 NUMERICAL MODELLING

Following relations are used to non-dimensionalise the governing equations.

x°	$=$	$\frac{x}{l_3}$	Non-dimensional depth	(3.50)
t°	$=$	$\frac{\alpha t}{l_3^2}$	Non-dimensional time	
T°	$=$	$\frac{KT}{H_a l_3}$	Non-dimensional temperature	
H_s°	$=$	$\frac{H_s}{H_a}$	Non-dimensional solar radiation	
P°	$=$	$\frac{P}{P_t}$	Non-dimensional pressure	

Superscript '°' is used to denote the non-dimensional form. On substituting the above relations of eqn. (3.50) into eqns. (3.21), (3.31), (3.38) and (3.43), and simplifying, the respective governing equations take the following form.

$$z_1 \frac{\partial T_u^\circ}{\partial t^\circ} = \frac{\partial T^\circ}{\partial x^\circ} \Big|_{z_1} + \tau H_s^\circ (1 - h_{l_1}) - \frac{h_c l_3}{K} (T_u^\circ - T_a^\circ) - \beta (T_u^\circ - T_{sky}^\circ)^4 - \gamma (P_s^\circ - P_a^\circ) \quad (3.51)$$

$$\frac{\partial T^\circ}{\partial t^\circ} = \frac{\partial^2 T^\circ}{\partial x^\circ^2} + \tau b \frac{H_s^\circ}{x^\circ} \quad (3.52)$$

$$(1 - z_2) \frac{\partial T_L^\circ}{\partial t^\circ} = h_2 \tau H_s^\circ - \frac{\partial T^\circ}{\partial x^\circ} \Big|_{z_2} - \frac{K_G}{K} \frac{\partial T_G^\circ}{\partial x^\circ} \Big|_{1.0} - \eta \quad (3.53)$$

and

$$\frac{\partial T_G^\circ}{\partial t^\circ} = \left(\frac{\alpha_G}{\alpha} \right) \frac{\partial^2 T_G^\circ}{\partial x^\circ 2} \quad (3.54)$$

Where,

$$z_1 = l_1/l_3 \quad (3.55a)$$

$$z_2 = l_2/l_3 \quad (3.55b)$$

$$\beta = \frac{\epsilon \sigma F_s l_3^4 H_a^3}{K^4} \quad (3.55c)$$

$$\eta = \frac{\alpha_e}{H_a} \quad (3.55d)$$

$$\gamma = \frac{\lambda h_c}{1.6 C_s H_a} \quad (3.55e)$$

Similarly on non-dimensionalising, the boundary conditions can be written as:

$$T_u^\circ = T_a^\circ \quad \text{for all } t^\circ \geq 0 \quad (3.56)$$

$$T^\circ(x) = T_u^\circ \quad \text{at } x^\circ = z_1, t^\circ \geq 0 \quad (3.57)$$

$$T^\circ(x) = T_L^\circ \quad \text{at } x^\circ = z_2, t^\circ \geq 0 \quad (3.58)$$

$$T_G^\circ = T_L^\circ \quad \text{at } x^\circ = 1.0, t^\circ \geq 0 \quad (3.59)$$

$$T_G^\circ = T_a^\circ \quad \text{at } x^\circ = 1.0 + \frac{l_0}{l_3}, t^\circ \geq 0 \quad (3.60)$$

and

$$\begin{aligned}
 T_u^{\circ} &= T_a^{\circ} \\
 T^{\circ}(x) &= T_a^{\circ} \\
 T_L^{\circ} &= T_a^{\circ} \\
 T_G^{\circ} &= T_a^{\circ}
 \end{aligned}
 \quad \text{at } t^{\circ} = 0 \quad (3.61)$$

It is very tedious and time consuming to solve the governing equations analytically. However, their finite difference analogues can be solved easily. For writing the finite difference equations Crank - Nicolsen [27, 28, 29] scheme has been utilized. The governing equations then assume the form as given below. The superscript '°' used to represent the non-dimensional form is being dropped for convenience.

$$\begin{aligned}
 T_u^{n+1} &= T_u^n + \left(\frac{\Delta t}{Z_1} \right) \left[\frac{\partial T}{\partial x} \Big|_{Z_1} + \tau^n H_s^n (1 - h_{11}) \right. \\
 &\quad - \frac{h_c l_3}{K} (T_u^n - T_a^n) - \beta (T_u^{n4} - T_{sky}^{n4}) \\
 &\quad \left. - \gamma (P_s^n - P_a^n) \right] \quad (3.62)
 \end{aligned}$$

$$\begin{aligned}
 -r T_{i-1}^{n+1} + 2 (1 + r) T_i^{n+1} - r T_{i+1}^{n+1} &= r T_{i-1}^n \\
 + 2 (1 - r) T_i^n + r T_{i+1}^n + \frac{2 \tau^n b}{i} \left(\frac{\Delta t}{\Delta x} \right) H_s^n \quad (3.63)
 \end{aligned}$$

$$T_L^{n+1} = T_L^n + \left(\frac{\Delta t}{1 - z_2} \right) \left[h_2 \tau^n H_s^n - \left. \frac{\partial T}{\partial x} \right|_{z_2}^n \right. \\ \left. - \frac{K_G}{K} \left. \frac{\partial T_G}{\partial x} \right|_{1.0}^n - \eta \right] \quad (3.64)$$

and

$$-s T_{j-1}^{n+1} + 2(1+s) T_j^{n+1} - s T_{j+1}^{n+1} = s T_{j-1}^n \\ + 2(1-s) T_j^n + s T_{j+1}^n \quad (3.65)$$

$$\text{Where } r = \Delta t / \Delta x^2 \quad (3.66a)$$

$$s = \frac{\alpha_G}{\alpha} \cdot \frac{\Delta t}{(\Delta x)^2} \quad (3.66b)$$

Superscript 'n' depicts the time level and subscript 'i' and 'j' represent the space level in the NCZ and in the ground, respectively. The above finite difference equations represent the numerical model of the solar pond.

3.6 THE COMPUTER PROGRAM

Eqns (3.62), (3.63), (3.64) and (3.65) were numerically solved on the computer, HP 9000/850 system. The following paragraphs are devoted to the explanation of the development of the program.

The model employs a thermal network that divides the solar pond into horizontal sublayers. The NCZ is divided

into sublayers each with depth of 0.1 m while the UCZ and LCZ are one sublayer each as there is no variation of temperature with depth in the UCZ and the LCZ. Network nodes are located in the middle of each sublayer and the node for the ambient temperature is at the top of the pond. Nodes of adjacent sublayers are in conductive thermal contact and the temperature variation between nodes is assumed to be linear. Physical parameters are assumed to be constant throughout each sublayer.

Since hourly temperature, solar insolation and RH data for New Delhi were available, the time interval for iteration was taken as one hour. The computer was fed with one full year solar insolation data beginning from January 1st.

The pond depth, thickness of the NCZ, the thickness of the UCZ, and thermophysical properties of the salt solution and the ground, were given as input to the program.

The first few steps of the program have been devoted to the conversion of the variables into non-dimensional form and development of tria-diagonal matrices required for the Eqn. (3.63) and (3.65). Calculation of the angle of incidence using the latitude of the location, time of the day and day of the year plus the computation of the coefficient of transmission using fresnel's relations have also been included in the program.

The tria-diagonal matrices are decomposed into the upper and the lower triangular matrices. Eqsns. (3.62), (3.63), (3.64) and (3.65) are then solved with iterated value of gradients. The output of the program is obtained in the form of the temperature of LCZ at every 350 hour internal. The program was run for a number of heat extraction loads on the pond with variable days for the application and removal of loads.

CHAPTER 4

RESULTS AND DISCUSSIONS

4.1 EFFECT OF TRANSMISSION COEFFICIENT

The model developed in this thesis compares the effect of transmission coefficient on the temperature rise of the LCZ by calculating the angle of incidence, hence transmission coefficient, at each hour of the year, with a constant transmission coefficient, corresponding to 2 PM solartime at equinox [29] ($\tau = 0.979$), throughout the year. With a constant transmission coefficient of 0.979, the LCZ temperature is slightly on the higher side than with a variable transmission coefficient. The maximum temperature difference of about 8°C occurs at the end of the year.

Figs. 4.1(a) and 4.1(b) show the variation of transmission coefficient with time. It can be seen from the figures that between 10 to 14 hrs of the day, the transmission coefficient has nearly a constant value for each month of the year varying slightly over the months. Fig. 4.1(b) also displays that τ increases upto the month of July each year and then starts decreasing. The maximum variation in τ , at solar noon is from 0.961 to 0.979 in a year. Thus employing a

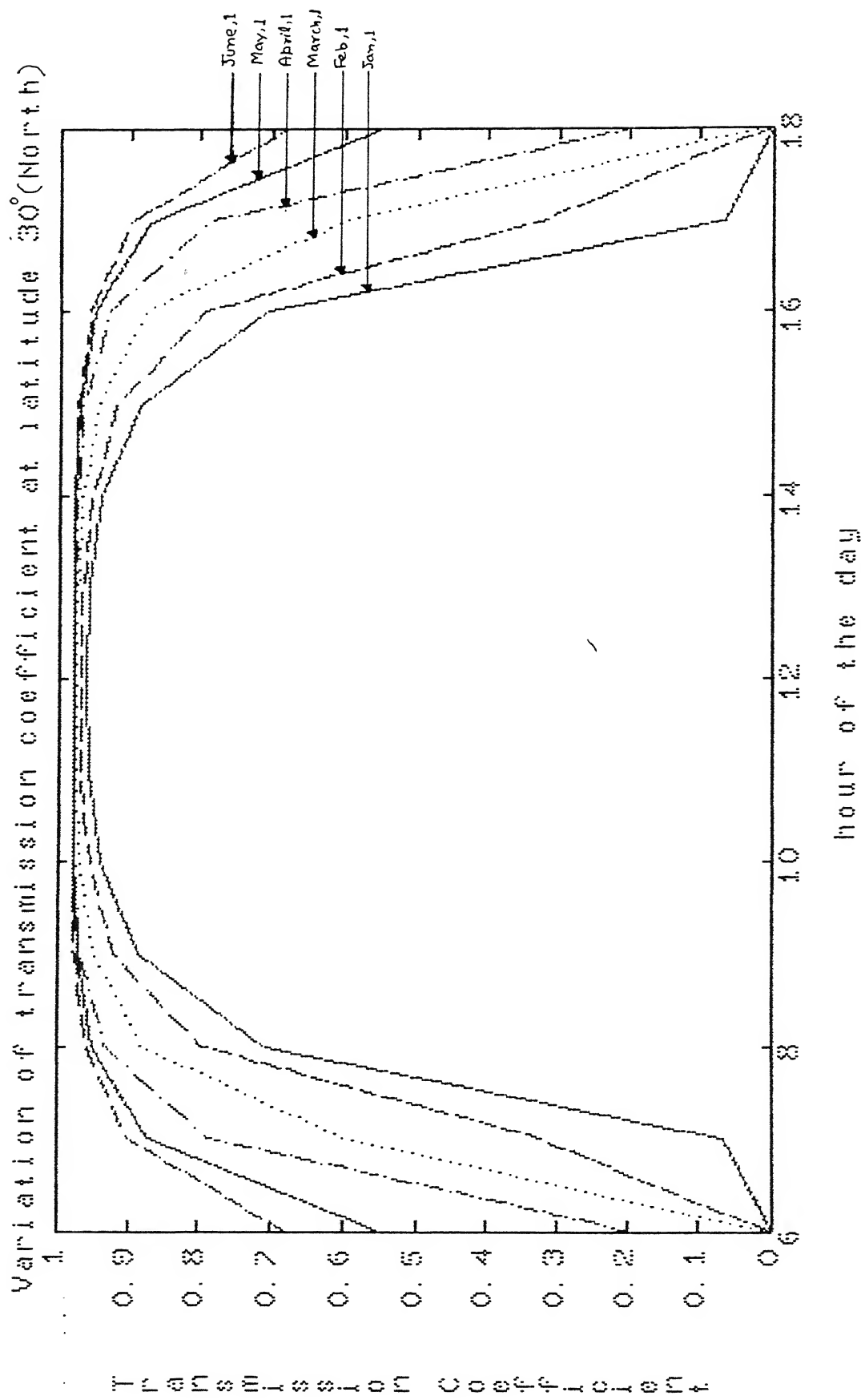


Fig. 4.1(a) : Variation of transmission coefficient for the first six months of the year.

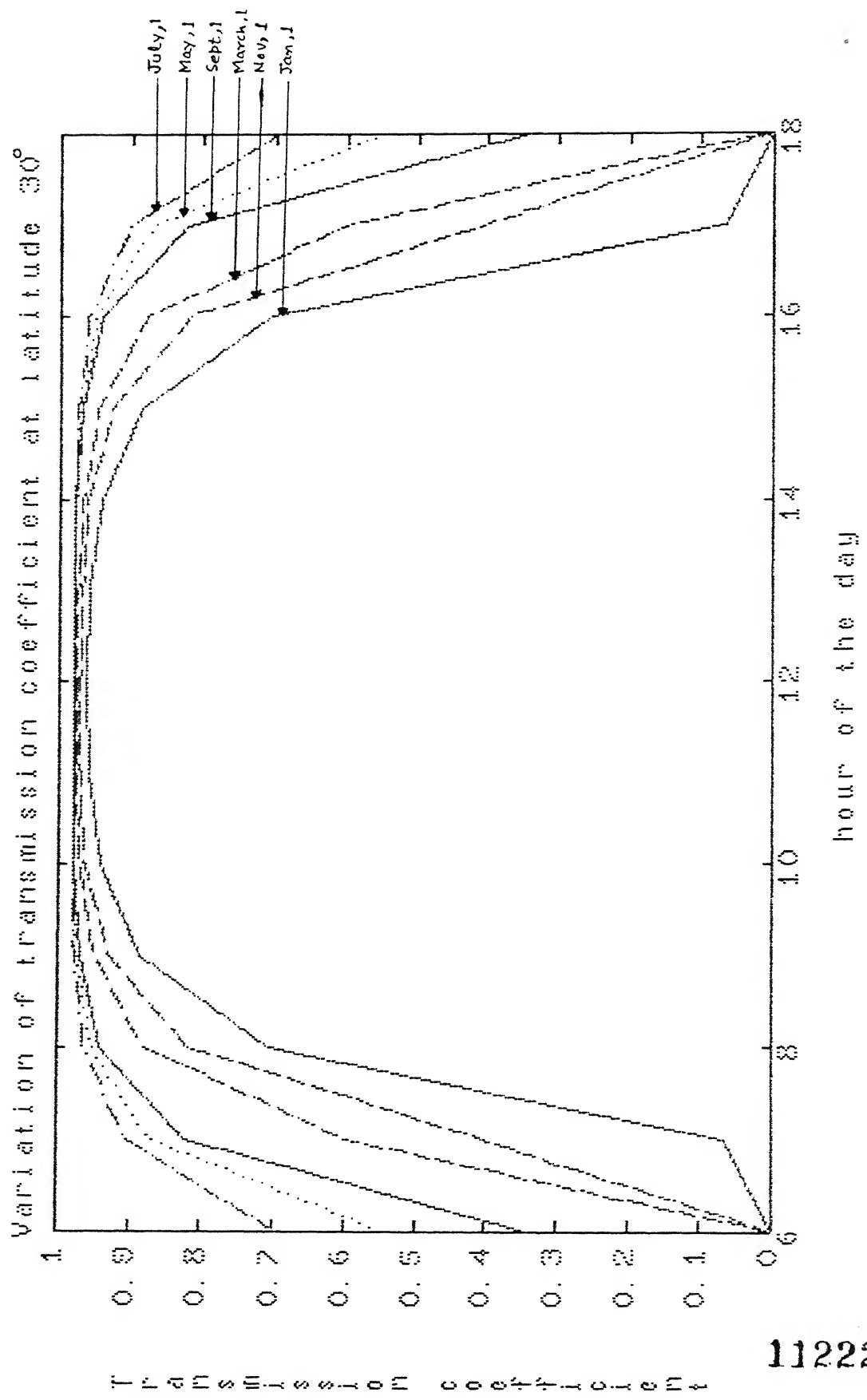


Fig. 4.1(b): Variation of transmission coefficient for the whole year.

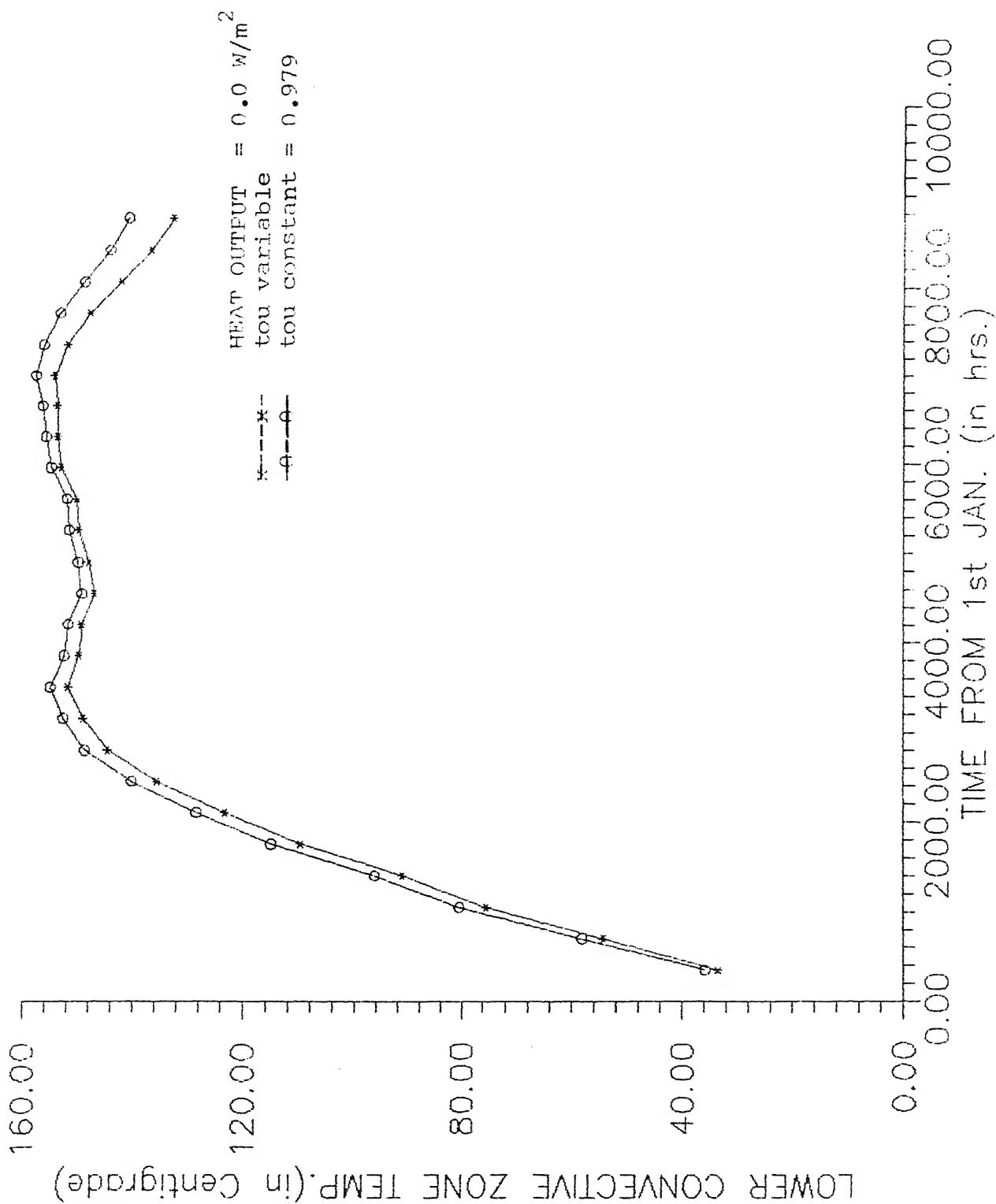


Fig. 4.2: Effect of on LCC temperature.

constant value of $\tau = 0.979$ leads to higher values of LCZ temperature. This can be seen clearly in Fig. 4.2 which gives the LCZ temperature variation with time using variable and constant transmission coefficients. This is in full agreement with the findings of J.R. Hull [29] that hourly variation of transmission coefficient over the year has very little effect on the pond's overall performance.

4.2 EFFECT OF EVAPORATION LOSS

Fig. 4.3 shows the effect of evaporation loss from the pond surface. Lower curve depicts the LCZ temperature variation when all the losses from the pond i.e., convection, radiation, evaporation and ground losses have been considered. Upper curve gives the LCZ temperature when all but evaporation losses have been taken into account. It can be seen from the graph that around 4200 hr i.e., during June, evaporation loss reaches a maximum. This explains the dip in the lower curve despite the fact that solar radiation during this period is maximum. As the evaporation loss reduces with time the temperature of the LCZ rises till approximately 7000 hr i.e., up to October end, after which it goes down again as radiation losses increase from the pond surface due to decreasing ambient temperature coupled with decreasing solar insolation. At the end of the year, the temperature difference in the LCZ under the above two circumstances is only 10°C , which is not very substantial. Evaporation loss, however, is predominant mainly for the three months beginning April.

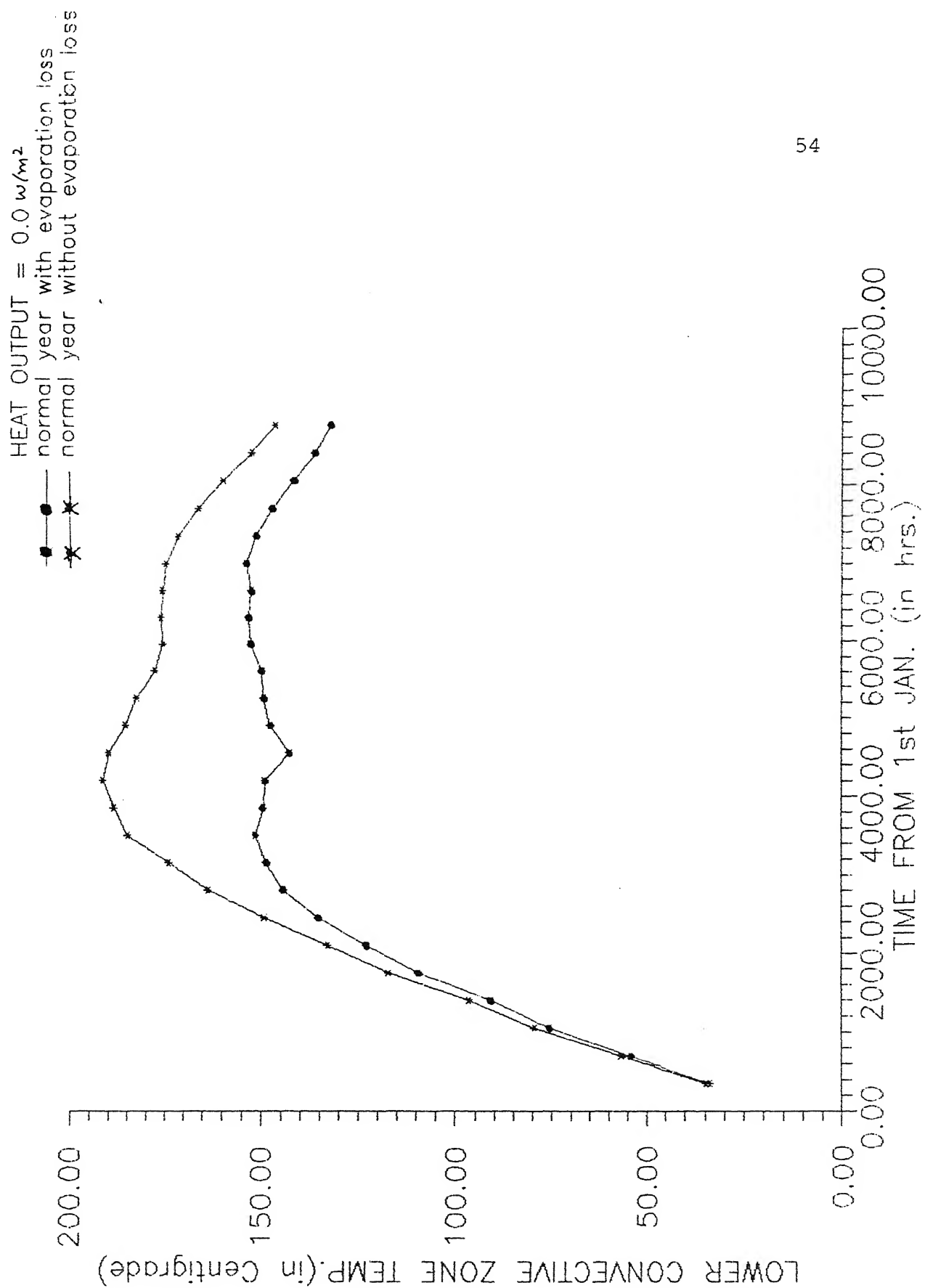


Fig. 4.3: Effect of evaporation loss on LCZ temperature.

4.3 EFFECT OF ONE MONTH OF CONSECUTIVE CLOUDY DAYS

In the present study, response of the solar pond to several consecutive cloudy days has also been investigated. This is quite important for the application of solar ponds for house heating, process heating and electrical power generation. It is assumed that July in the Indian sub-continent is fully cloudy and solar insolation for these 31 days is zero. The temperature rise of the pond is plotted for such an exceptional year and is compared with a normal year in Fig. 4.4 for the case of no heat extraction from the pond. It is observed that at the end of thirty one consecutive cloudy days, the temperature of the LCZ reduces to a minimum of about 105°C . This is followed by a period of warming up as the consecutive cloudy period ends and solar radiation starts coming in. The temperature of the LCZ further decreases as the winter sets in. At the end of the year, the temperature difference of the pond for a normal and an exceptional year of 31 consecutive cloudy days is less than 5°C . From the results of Fig. 4.4 it is concluded that solar ponds are relatively reliable solar collector-cum-storage systems, since even in an extreme case of thirty one consecutive cloudy days, with zero solar energy influx, only slightly reduced LCZ temperatures are available at the end of the year. It is of course clear that probability of having thirty one consecutive cloudy days is almost zero. Even for a cloudy day the solar radiation available is almost 15 to 20 percent of a corresponding sunny day.

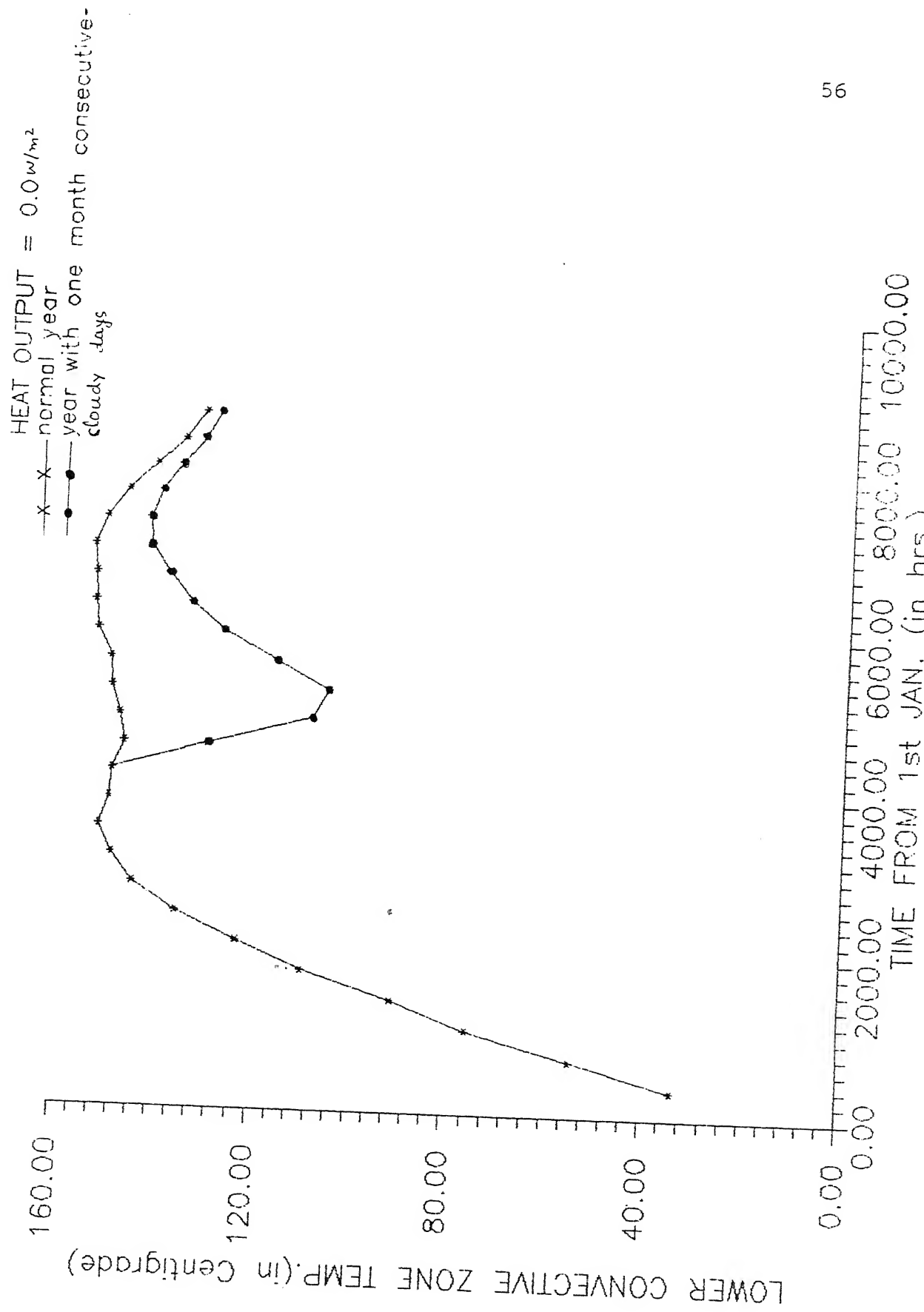


Fig. 4.4: Effect of one month of consecutive cloudy days on

4.4 EFFECT OF WATER QUALITY OF THE SOLAR POND

In Fig. 4.5, the effect of pond water clarity on LCZ temperature is shown. The upper curve is for the condition when W_{qf} for the pond water is unity i.e., ideally clear water and the lower curve for the condition when $W_{qf} = 0.75$ i.e., a condition of practically clear water at which pond could be maintained. Due to dirt, floating organic matter, algae growth etc. the direct solar radiation component penetration into the pond is reduced and the diffused radiation component is augmented due to partial scattering of the beam component of radiation. At 6500 hrs for the water quality curve of 0.75, the peak temperature is reduced approximately 20°C. It is clear from the figure that for practical ponds, the LCZ temperature is appreciably lower throughout the year than for the ideal water ponds. This suggest that for higher LCZ temperatures, a higher operating cost is expected for maintaining the clarity of the pond water near about unity.

4.5 EFFECT OF HEAT EXTRACTION ON SOLAR POND

A detailed analysis of solar pond performance under variable conditions of load, load application day and load removal day has been carried out. For all the cases, all the losses and ideal water quality have been taken into account. After an initial warm up period, a fixed percentage of the

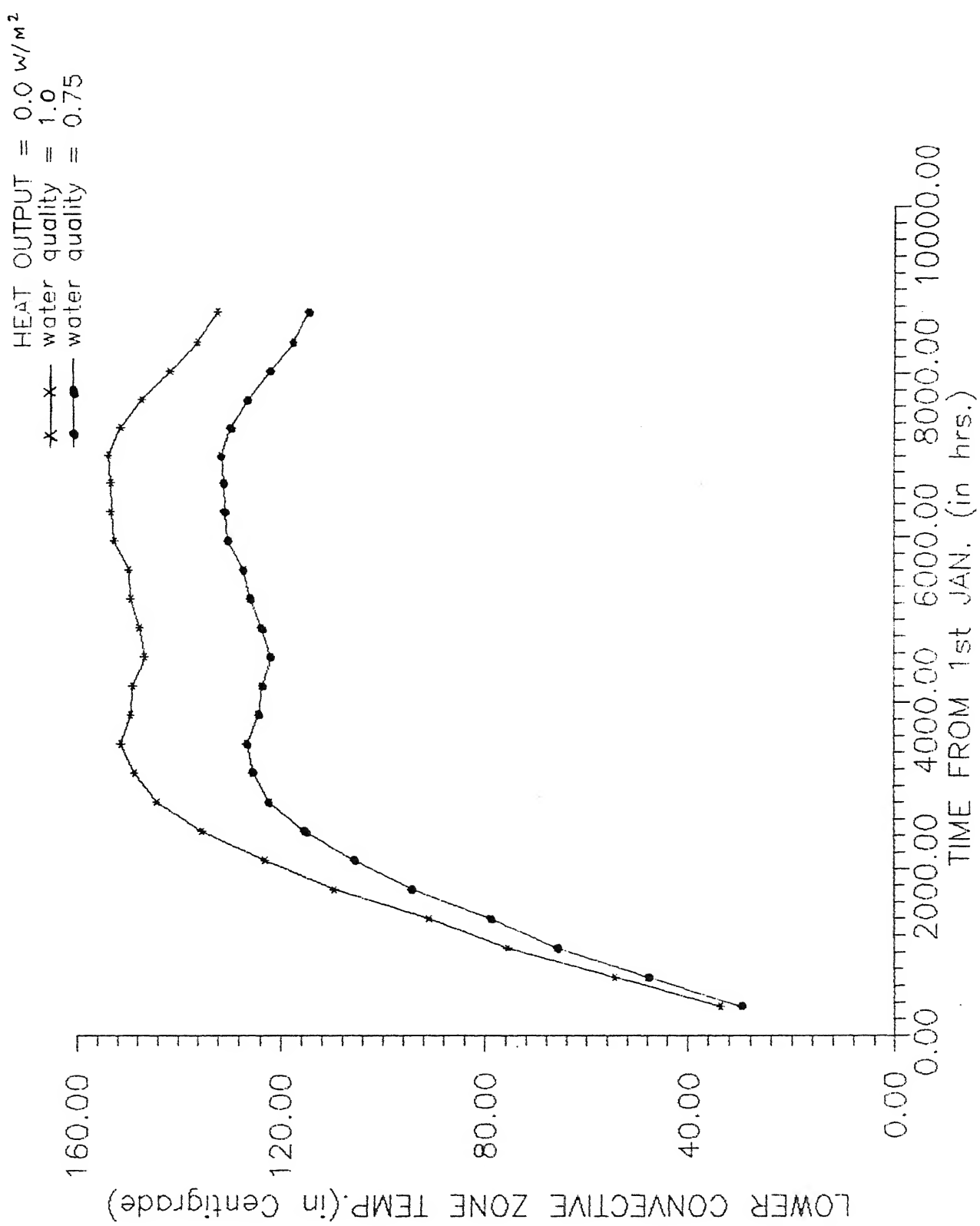


Fig. 4.5: Effect of water quality on LCZ temperature.

annual mean solar radiation is assumed to be removed continuously from the pond at its bottom. It is assumed that heat extraction process does not produce any instability in the pond.

Fig. 4.6, depicts the case when load is applied after an initial warming up period of sixty days, at the rate of 20, 40, 60, and 80 W/m^2 throughout the year. As the rate of heat removal increases, the pond temperature drops considerably. Therefore, for a practical pond operation, the rate of heat removal should be such that the temperature of the pond is maintained at a reasonable level. At the end of 60 days, the LCZ temperature reached nearly 90°C . For the loads of 20, 40, and 60 W/m^2 , the LCZ temperature goes on increasing, the increase being less for the higher loads. This is explained by the fact that solar input at these loads, is more than the total heat extraction (inclusive of all losses). However, for the 80 W/m^2 load, the LCZ temperature does not rise further as the solar input at this load is less than the total heat loss.

Fig. 4.7 portrays the case when LCZ has already attained its maximum possible temperature after initial 180 days of heating. Next the solar input starts decreasing while the total load is increasing due to lower surrounding temperatures. As negative temperature gradient has already set in, the increasing load rate enhances the temperature drop rate throughout the year.

Fig. 4.8 depicts the case when the load application day is the 180th and load is removed on 300th day of the year, so that during the winter period pond can regain some lost temperature. Curves show a rising trend after 7200 hrs because due to lower temperature of the pond, the losses are reduced. Hence solar input is more than the losses from the pond. Fig. 4.8 also suggests that we can expect a higher rate of heat removal for a small period still maintaining a practical pond temperature.

Figs. 4.9 and 4.10 show the case of the load application day as 240th and the load removal day as 365th and 300th day, respectively. These figures suggest that it is not advantageous to increase the day of application of load as the useful days of pond's operation (days of heat extraction) narrow down without any compensating advantage. Further a high pond temperature easily destabilises the pond due to starting of boiling which is not permissible in an actual solar pond. It is clear that for practical operation of a solar pond, excessive heat must be removed as useful heat for various applications. Water should not be allowed to boil since it will destroy the salt gradient and hence the NCZ.

4.6 CONCLUSIONS

Based on the results obtained from the present computer simulation of the performance of solar ponds in the northern part of India it appears that solar ponds are reliable

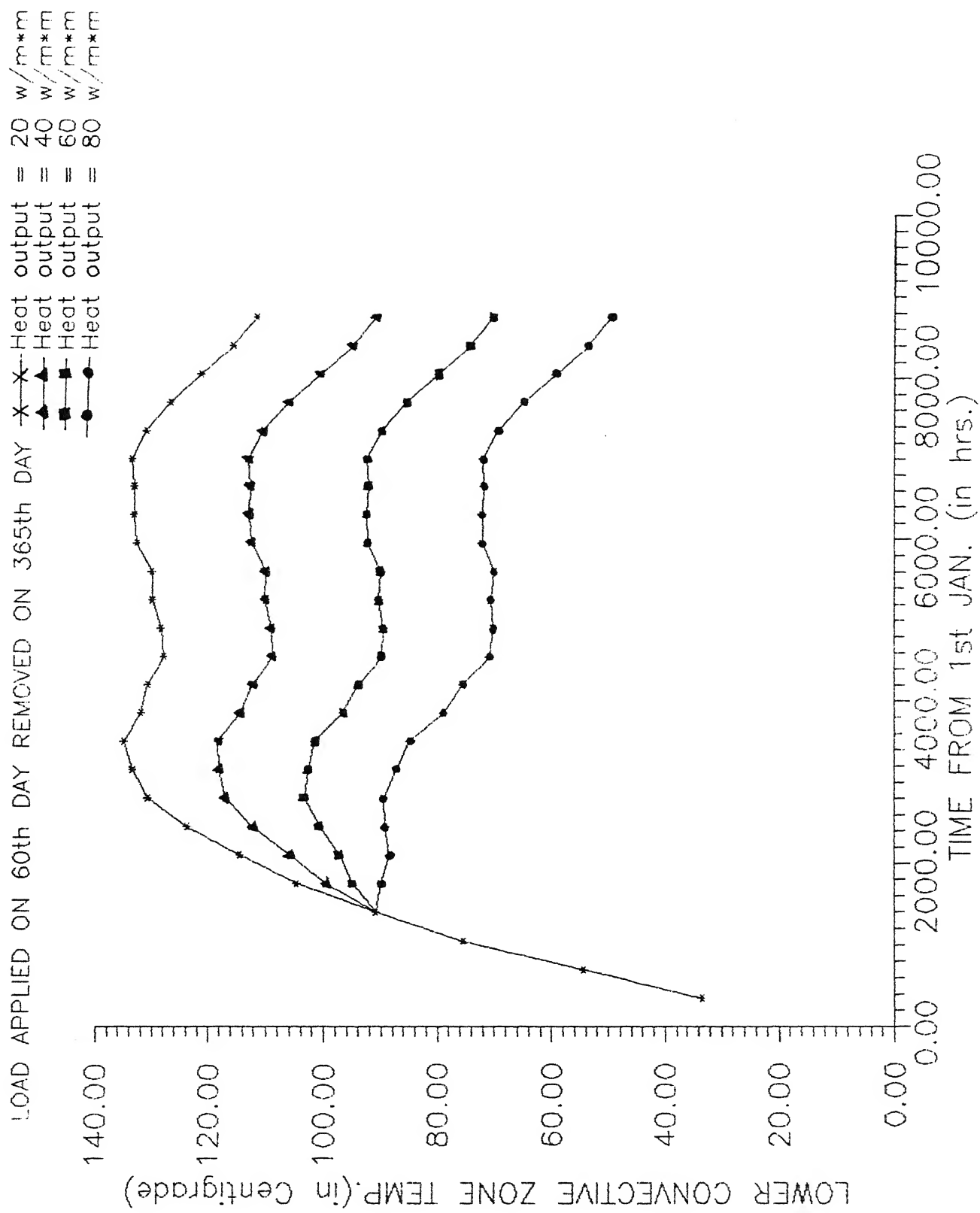


Fig. 4.6: LCZ temperature with the load applied on the 60th day and load removed on the 365th day.

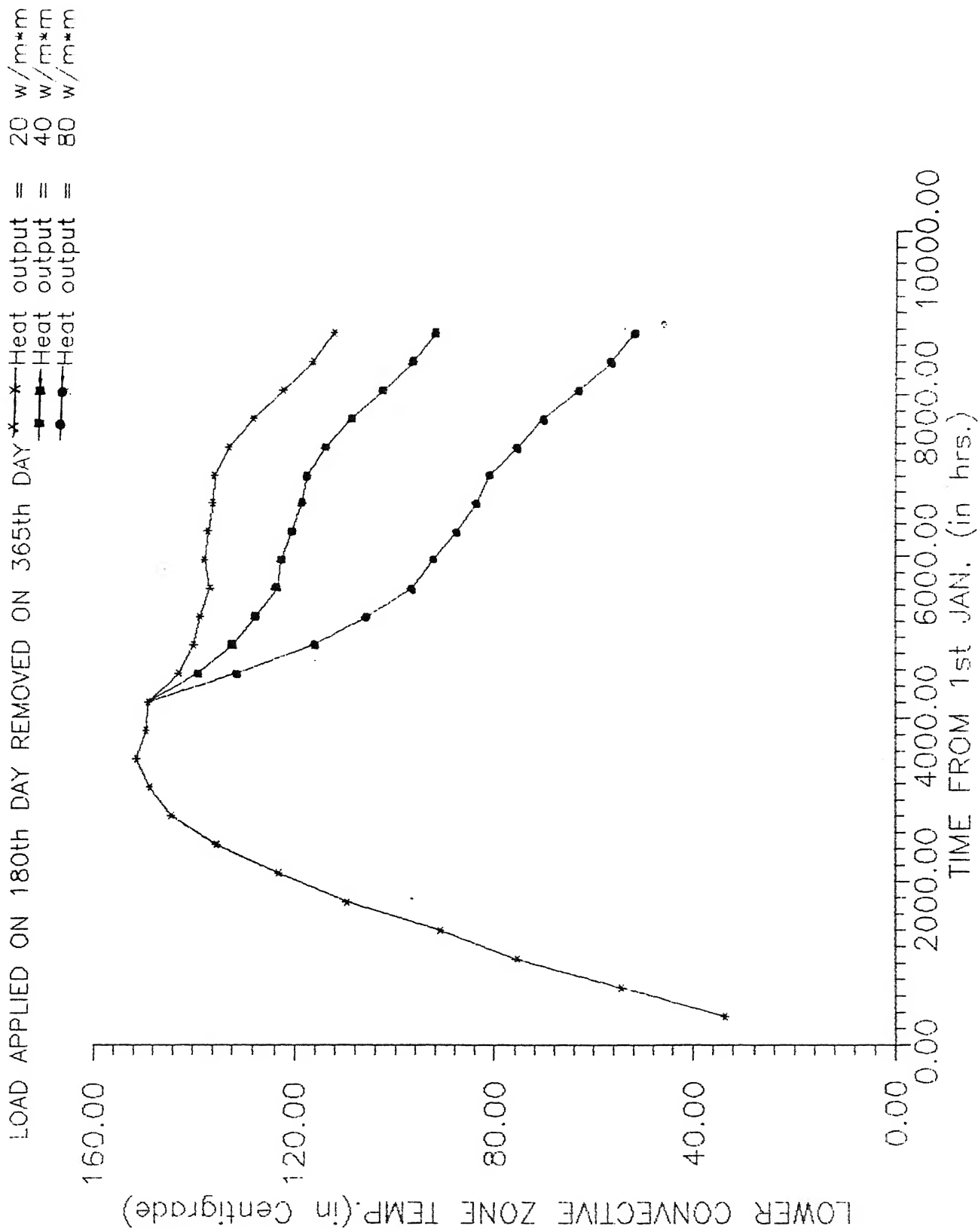


Fig. 4.7: LCZ temperature with the load applied on the 180th day and load removed on the 365th day.

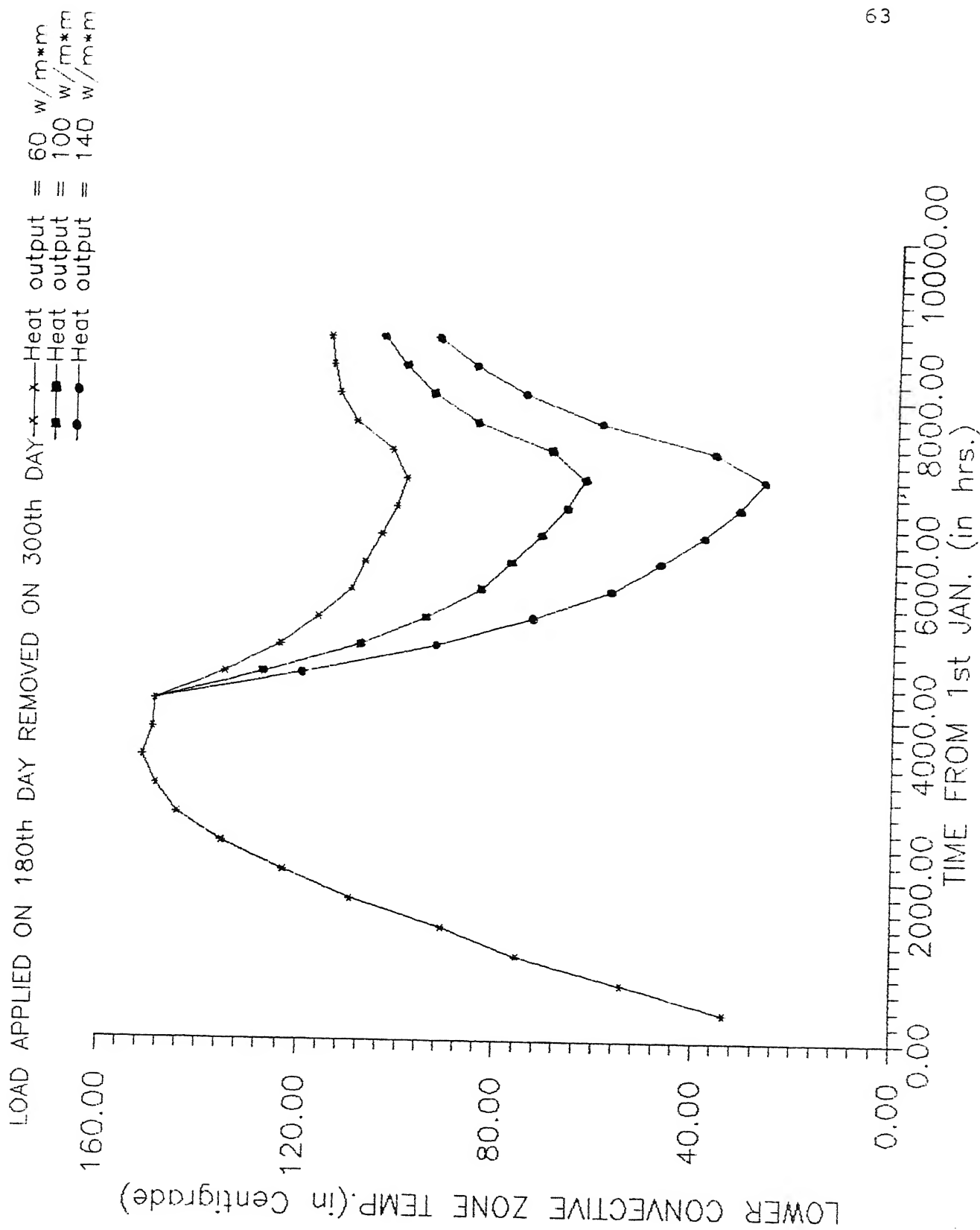


Fig. 4.8: LCZ temperature with the load applied on 180th day, removed on 300th day.

LOAD APPLIED ON 240th DAY REMOVED ON 365th DAY

Heat output = 20 w/m²m
Heat output = 40 w/m²m
Heat output = 80 w/m²m
Heat output = 100 w/m²m

160.00

120.00

80.00

40.00

LOWER CONVECTIVE ZONE TEMP. (in Centigrade)

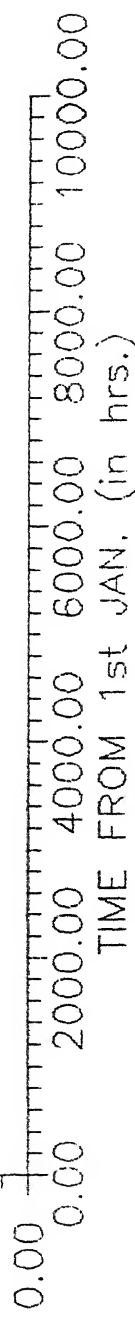


Fig. 4.9: LCZ temperature with the load applied on 240th day, removed on 365th day.

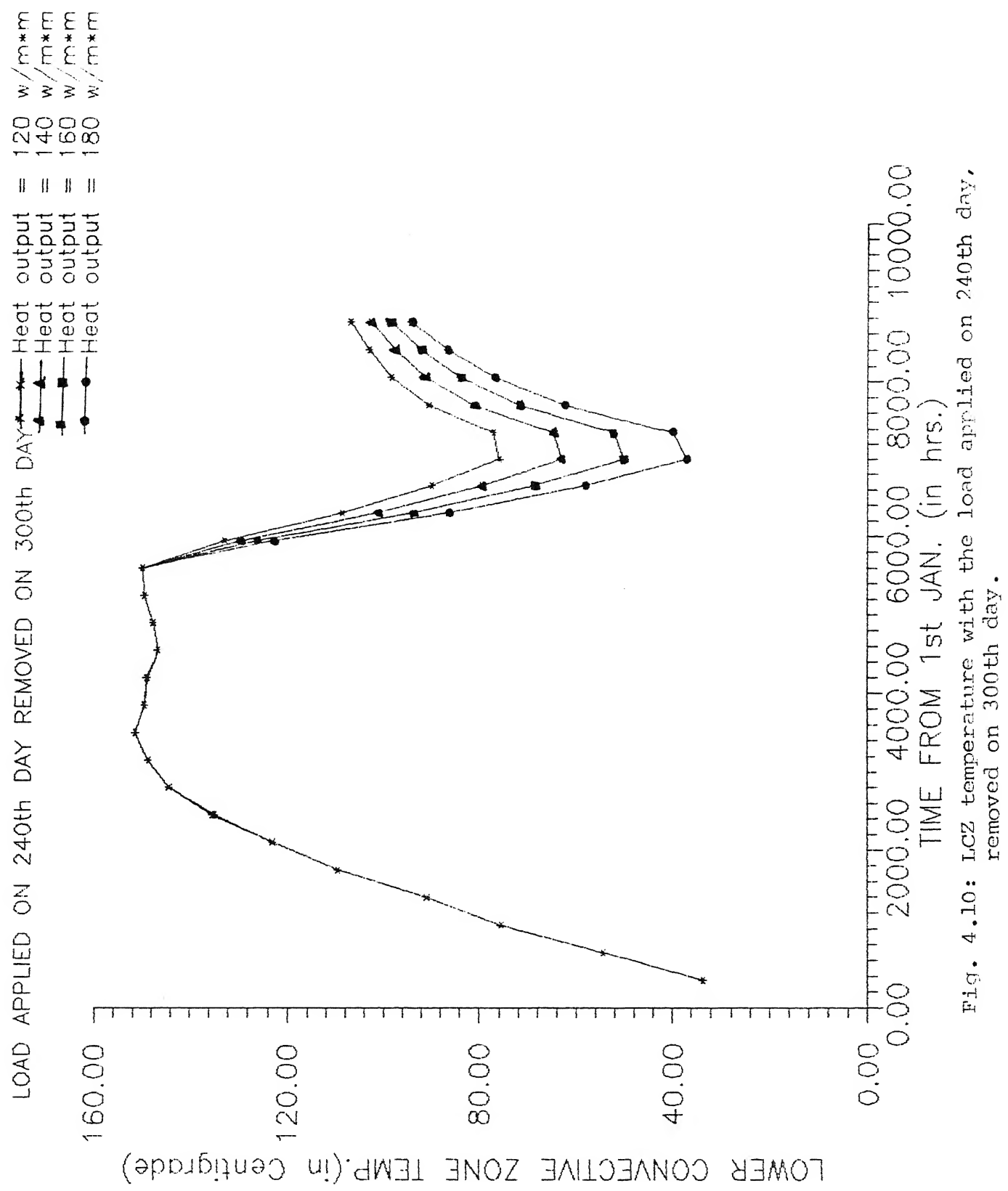


FIG. 4.10: LCZ temperature with the load applied on 240th day, removed on 300th day.

solar collectors for production of hot water all year round in this area. As can be seen from Fig. 4.2, the temperature at the bottom of a 1.5 m deep pond whose operation starts on Jan 1, rises rapidly and reaches a value of 150°C in May with no load conditions.

Heat should be extracted from the pond to the extent that boiling does not occur which would disturb the salt concentration gradient.

Furthermore, it was observed that water clarity significantly affects the pond temperature rise throughout the period of operation and for better overall performance, water of the pond should be made free from dirt, algae organic matter etc.

Variable τ has little affect on the pond overall performance in comparison to the constant τ .

The evaporation loss from the surface of a solar pond is quite significant during the months of May, June and July.

Study of several consecutive cloudy days shows that solar ponds offer a relatively reliable solar collector-cum-storage system.

4.7 SUGGESTION FOR FURTHER WORK

The present study is basically a theoretical investigation into the performance of salt gradient solar ponds. The next logical step towards extension of the present work would be to construct and study an experimental pond to verify the results and also to relax some of the assumptions underlying the present investigation such as constant thermal conductivity, one dimensional conduction and constant water clarity with time.

REFERENCES

1. M.P. Agarwal, *Solar Energy*, S. Chand and Company Ltd., New Delhi (1985).
2. J.A. Duffie and W.A. Beckman, *Solar Energy Thermal Processes*, Wiley, New York (1974).
3. Karl W. Boer, *Advances in Solar Energy Vol. 4*, Americal Solar Energy Society, Inc. (1988).
4. H.P. Garg, S.C. Mullick and A.K. Bhargava, *Solar Thermal Energy Storage*, D. Reidel Publishing Company (1985).
5. S.L. Sargent, An overview of solar pond technology. *Proc. of The Solar Industrial Process Heat Transfer*, pp. 355-371 (1979).
6. J.R. Hull, Membrane stratified solar ponds. *Solar Energy*, 25, 317 (1980).
7. A.V. Kalecsinsky, Ueber die Ungarischen Warmen and Neissen Kochsalzseen als Natuerliche Waerm - eaccumulatoren. *Ann. Physik IV*, 7, 408 (1902).
8. H. Tabor and R. Matz, A status report on a solar pond project. *Solar Energy* 9, 177 (1963).

9. T.R.A. Davey, The Aspendale solar pond. CSIRO, Australia.
10. J. Hirschmann, Suppression of natural convection in open ponds by a concentration gradient. Report on U.N. Conference on New Sources of Energy, New York p. 478 (1962).
11. G.C. Jain, Heating of solar pond Proc, Paris Congress on Solar Energy, (1973).
12. K.N. Eliseev and U. Yu. Usmanov. Theoretical investigation of thermal regime of a solar pond. *Geliotekhnika* 7, 17 (1971).
13. A. Rabl and C.E. Nielsen, Solar ponds for space heating. *Solar Energy* 17, 1 (1975).
14. B. Saulnier, N. Chepurniy, S.B. Savage, and T.A. Lawand, Field testing of a solar pond. Extended Abstracts Int. Solar Energy Society. Los Angeles, (1975).
15. D.L. Styris, O.K. Harling, R.Z. Zaworski and J. Leshuk, The non-convecting solar pond applied to building and process heating. *Solar Energy* 18, 245 (1976).
16. G. Assaf, The Dead Sea: A scheme for a solar lake. *Solar Energy* 18, 293 (1976).

17. A Akbarzadeh and G. Ahmadi, "Under Ground Thermal Storage In the Operation of Solar Ponds", presented at the Seventh International Solar Energy Congress, January 16-21, (1978).
18. H. Weinberger, The physics of the solar pond. *Solar Energy* 2, 45 (1964).
19. C.F. Kooi, The steady state salt gradient solar pond. *Solar Energy* 23, 37 (1979).
20. M.M.A. Hawlader and B.J. Brinkworth, An analysis of the non-convective solar pond. *Solar Energy* 27, 195 (1982).
21. H. Tabor, Solar collector developments in Israel. *Solar Energy* 3, 8 (1959).
22. H.C. Bryant and I. Colbeck, A solar pond for London. *Solar Energy* 19, 321 (1977).
23. P.T. Tsilingiris, An accurate upper estimate for the transmission of solar radiation in salt gradient ponds. *Solar Energy* 40, 41 (1988).
24. H. Buctiberg and J.R. Roulet, Simulation and optimization of solar collection and storage for house heating. *Solar Energy* 12, 31 (1966).
25. R.H. Perry and C.H. Chilton (Eds.), *Chemical Engineers Hand Book*, 5th Edn., p. 12-2 Mc Graw-Hill, New York (1973).

26. V.V.N. Kishore and Veena Joshi, A practical collector efficiency equation for non-convecting solar ponds. *Solar Energy* 33, 391 (1984).
27. E. Carnahan, H.A. Luther and J.O. Wilkes, *Applied Numerical Methods*, Wiley, New York (1969).
28. R.D. Croft and L.G. David 'Heat Transfer Calculation by Finite Difference Equations', Applied Science Pub. Ltd., London 1977).
29. S.R. Hull, Computer simulation of a solar pond thermal behaviour. *Solar Energy* 25, 33 (1980).
30. A. Akbarzadeh and G. Ahmadi, Computer simulation of the performance of a solar pond in the southern part of Iran. Proc. of the ISEB Congress, New Delhi, 1181 (1978).
31. A. Mani, *Hand Book of Solar Radiation Data for India*.

APPENDIX ATHERMAL STABILITY OF SOLAR PONDS

Weinberger [18] has developed a one dimensional thermal model and explained the stability of solar ponds. SP will be stable, i.e. all the three zones remain present, when the density gradient on account of the salt concentration is equal or greater than the negative density gradient produced by the temperature or the total derivative of density with respect to depth is greater than or equal to 0.

$$\rho = f(c, T)$$

$$\frac{d\rho}{dx} = \left(\frac{\partial \rho}{\partial c}\right)_T \frac{dc}{dx} + \left(\frac{\partial \rho}{\partial T}\right)_c \frac{dT}{dx} \geq 0$$

$$\text{or } \frac{dc}{dx} = \frac{\beta_T}{\beta_s} \frac{dT}{dx}$$

Where,

$$\beta_T = \left(\frac{\partial \rho}{\partial T}\right)_{\rho}, \text{ Thermal expansion coefficient of water}$$

$$\text{and } \beta_s = \left(\frac{\partial \rho}{\partial c}\right) \frac{1}{\rho}, \text{ Salt expansion coefficient}$$

Integrating,

$$(\Delta c)_{\min} = \frac{\beta_T}{\beta_s} \Delta T$$

This expression relates the minimum concentration difference required to maintain thermal stability between two layers of liquid with ΔT temperature difference.

This equation ensures only thermal stability. In long run other kind of instability also occurs. This occurs because thermal diffusivity is much greater than molecular diffusivity. So that concentration fluctuations will last almost 100 times longer than temperature fluctuation. Some natural mechanisms also induce convection cells which grow with time. Unless all growth is prevented, it will eventually destroy the NCZ. To suppress oscillatory disturbances the salt concentration gradient should fulfil the following condition:

$$\frac{\partial C}{\partial x} \geq \left(\frac{P_r + 1}{P_r + s} \right) \frac{\beta_T}{\beta_s} \left(\frac{\partial T}{\partial x} \right)$$

Where $P_r = \frac{\nu}{\alpha T}$ Prandtl number

$$\tau_s = \frac{\alpha_s}{\alpha T} = \frac{\text{Coefficient of salt diffusivity}}{\text{Coefficient of thermal diffusivity}}$$

The minimum salt concentration required to prevent oscillatory disturbance is therefore

$$(\Delta C)_{\min} = \frac{P_r + 1}{P_r + s} \frac{\beta_T}{\beta_s} \Delta T$$

For a pond to remain stable for, considerably, longer period it is essential that,

- (a) Concentrated salt solution should be periodically added at the bottom to compensate for the loss of salt by diffusion.
- (b) The top of the pond should be frequently flushed to maintain a very low concentration of salt in top layers. This helps in maintaining the transparency of the pond.

APPENDIX BNOMENCLATURE

ABSI	Emissivity of the Pond surface
AK	Conductivity of salt solution
AKG	Conductivity of Ground
AL	Total depth of the pond
AL1	Depth of UCZ-NCZ interface
AL2	Depth of NCZ-LCZ interface
ALPHA	Thermal Diffusivity of salt solution
ALPHAG	Thermal Diffusivity of Ground
DELT	Time interval
DELTND	Non-dimensional time interval
DELK	Element thickness
DELKND	Non-dimensional element thickness
FS	Shape factor
GRADZ1	Temperature gradient at depth l_1
GRADZ2	Temperature gradient at depth l_2
GRADZ3	Temperature gradient at the bottom
HA	Annual average radiation
HC	Convective heat transfer coefficient
HS	Solar radiation
I	Number of sublayers in NCZ
IBP	Total number of days of operation

J Number of sublayers in the ground
TA Time of operation in Hrs.
NMA Day of application of load
NRE Day of removal of load
PHI Latitude of the place
QE Heat extraction rate
TA Ambient temperature
TALND Non-dimensional ambient temperature
TGND Non-dimensional ground temperature
TLND Non-dimensional LCZ temperature
TSKYND Non-dimensional sky temperature
TUND Non-dimensional UCZ temperature
TXND Non-dimensional NCZ temperature

APPENDIX C

```

      read(1,*)(rh1(iii,jjj),jjj=1,24)
80    continue
      read(1,*)qe
      gradz1=0.0
      gradz2=0.0
      gradz3=0.0
      sigma=5.67e-08
      beta=absi*fs*sigma*(al/ak)**4*ha**3
      r=delxnd/(delxnd*delxnd)
      s=r*alphag/alpha
      c
      h1=.75(.46-0.0953*log(al1))
      h1=(.46-0.0953*log(al1))
      h2=(0.46-0.0953*log(al2))
      c
      h2=.75(0.46-0.0953*log(al2))
      do 90 m=1,8
      a1(m,m)=2.0*r+2.0
      b1(m,m)=2.0-2.0*r
90    continue
      do 100 m=2,8
      a1(m-1,m)=-r
      a1(m,m-1)=-r
      b1(m-1,m)=r
      b1(m,m-1)=r
100   continue
      do 110 m=1,10
      a2(m,m)=2.0+2.0*s
      b2(m,m)=2.0-2.0*s
110   continue
      do 120 m=2,j
      a2(m-1,m)=-s
      a2(m,m-1)=-s
      b2(m-1,m)=s
      b2(m,m-1)=s
120   continue
      do 111 nn=2,2760
      inn=nn/24
      en=nn
      einn=inn
      tnn=en/24.0
      trnn=tnn-einn
      me=i+inn
      ame=me
      dol=24.0*trnn
      dol1=dol-1
      nm=nn-1
      iday=int(nn/24)
      ihr=nn-24*iday+1
      rh(nn)=rh1(iday,ihr)/100
      if(dol.le.6.0)goto 618
      if(dol.ge.18)goto 618
      pi=3.141569
      omega=(pi/12.0)*(dol-12.0)
      delta=23.45*sin(2.0*pi*(284.0+ame)/365.0)
      deltar=delta*pi/180.0
      phir=pi*phi/180.0
      cosin=sin(deltar)*sin(phir)+cos(deltar)*cos(phir)*cos(omega)
      ainc1=acos(cosin)
      sinin=sin(ainc1)
      sinre=sinin/1.33
      ref=asin(sinre)
      asr=ainc1-ref
      apr=ainc1+ref
      rtou=0.5*(sin(asr)/sin(apr))**2*(1.0+(cos(apr)/cos(asr))**2)
      tou=1-rtou
      tou=0.777
      go to 617
      c

```

```

618  tou=0.0
619  nm=nn-1
      if(me.lt.nma)go to 130
      if(me.gt.nme)go to 130
      eta=qe/ha
      go to 140
130  eta=0.0
140  do 222 id=1,2
      lemda=2300
      cs=1.0216
      iday1=iday+1
      ihr1=ihr-2
      tta=ta(iday1,ihr1)
      pa=rh(nm)*exp(18.403-3885/(tta+230))/760.0
      ps=pa/rh(nm)
      gama=lemda*hc/(ha*cs*760)
      tundn=tundo+(deltn/zi)*(gradz1-(hc*al/ak)*(tundo-talnd(nm))-
      1beta*(tundo**4-tskynd(nm)**4)+tou*dsc(nm)*(1.0-h1)-gama*(ps-pa))
      tlndn=tlndo+(deltn/(1.0-z2))*(h2*tou*dsc(nm)-gradz2-(akg/ak)
      1*gradz3-eta)
      do 150 ij=1,8
      ji=1
      b1t(ij,ji)=0.0
      do 150 k=1,8
      b1t(ij,ji)=b1t(ij,ji)+b1(ij,k)*txnd(k)
150  continue
      si=0.18*tou*deltn*dsc(nm)/delxnd
      do 160 k=1,8
      ak=k
      c1(k)=0.0
      sip(k)=si/ak
160  continue
      c1(1)=r*(tundo+tundn)
      c1(i)=r*(tlndo+tlndn)
      do 170 in=1,8
      ji=1
      rhsi(in)=b1t(in,ji)+sip(in)+c1(in)
170  continue
      a1l(1,1)=a1(1,1)
      a1u(1,1)=1.0
      do 180 l=2,8
      a1l(1,l-1)=a1(1,l-1)
      a1u(1,l)=1.0
      a1u(1-1,1)=a1(1-1,1)/a1l(1-1,1-1)
      a1l(1,1)=a1(1,1)-a1l(1,l-1)*a1u(1-1,1)
180  continue
      y1(1)=rhsi(1)/a1l(1,1)
      do 190 m=2,8
      y1(m)=(rhsi(m)-a1l(m,m-1)*y1(m-1))/a1l(m,m)
190  continue
      txnd(i)=y1(i)
      mn=8-i
      do 200 k=1,mn
      min=8-k
      mp=min+1
      txnd(min)=y1(min)-txnd(mp)*a1u(min,mp)
200  continue
      do 210 k= 1,10
      b2t(k,1)=0.0
      do 210 l=1,10
      b2t(k,l)=b2t(k,1)+b2(k,l)*tgnd(l)
210  continue
      do 220 k=1,10
      c2(k)=0.0
220  continue
      c2(1)=s*(tlndo+tlndn)

```

```

c2(j)=s*(ta1nd(nn)+ta1nd(nn))
do 230 k=1,10
kj=1
rhs2(k)=b2t(k,kj)+c2(k)
230  continue
a21(1,1)=a2(1,1)
a2u(1,1)=1.0
do 240 k=2,10
a21(k,k-1)=a2(k,k-1)
a2u(k,k)=1.0
a2u(k-1,k)=a2(k-1,k)/a21(k-1,k-1)
a21(k,k)=a2(k,k)-a21(k,k-1)*a2u(k-1,k)
240  continue
y2(1)=rhs2(1)/a21(1,1)
do 250 k=2,10
y2(k)=(rhs2(k)-a21(k,k-1)*y2(k-1))/a21(k,k)
250  continue
tgnd(j)=y2(j)
mo=10-1
do 260 k=1,mo
nim=10-k
np=nim+1
tgnd(nim)=y2(nim)-tgnd(np)*a2u(nim,np)
260  continue
gradz1=(gradz1+(ta1nd(nn)-txnd(1))/delxnd)/2.0
gradz2=(gradz2+(txnd(i)-txnd(i-1))/delxnd)/2.0
gradz3=(gradz3+(tgnd(2)-tgnd(1))/delxnd)/2.0
222  continue
tund=tundn
tindn=tindn
ian=nn/350.0
ann=nn
an=ann/350.0
if(ian.eq.an) goto 270
goto 280
270  write(2,11)nn
11   format(5x,'nn='15,/)
ak=.563
write(2,22)(tindn*ha*ai/ak-273)
22   format(5x,'lower convective zone temperature ='15.2,/)
gradz1=(txnd(2)-txnd(1))/delxnd
gradz2=(txnd(i)-txnd(i-1))/delxnd
gradz3=(tgnd(2)-tgnd(1))/delxnd
111  continue
close(unit=1)
stop
end

```

CC
 C INPUT DATA FILE C
 C FOR C
 C EFFECT OF VARIOUS PARAMETERS ON THE PERFORMANCE C
 C OF SALINITY GRADIENT SOLAR POND C
 C C
 C APPENDIX D TOSESH K. GUPTA C
 C CCC

1.5 0.2 1. AL,AL1, AL2
 35.641 .569 .519 HC,AK,AKG
 1.481e-07 1.0357e-06 228 ALPHA, ALPHAG, HA
 0.95 ABSI,
 1.0 28.5 FS,PHI
 8 I
 10 J
 6760 0.1 3600 365 NA,DELX,DELT,IBP
 366 366 NME,NMA
 AVE SOLAR RAD. IN JAN,FEB,MAR,APR,MAY,JUN,JUL,AUG,SEP,OCT,NOV,DEC
 0. 4. 96. 271. 433. 556. 618. 615. 552. 430. 268. 99. 5. 0.
 0. 20. 163. 364. 540. 670. 727. 728. 659. 534. 358. 165. 21. 0.
 1. 66. 260. 475. 655. 781. 845. 844. 769. 635. 458. 249. 64. 1.
 10. 130. 339. 554. 727. 848. 910. 903. 833. 699. 523. 318. 122. 10
 30. 177. 383. 581. 746. 865. 925. 920. 844. 719. 547. 352. 158. 27
 36. 164. 339. 510. 657. 758. 809. 813. 750. 639. 483. 318. 159. 36
 26. 130. 275. 425. 549. 640. 672. 671. 606. 518. 412. 273. 141. 32
 12. 101. 243. 392. 512. 607. 640. 659. 595. 510. 392. 255. 107. 13
 3. 79. 248. 431. 587. 698. 757. 747. 689. 571. 417. 244. 74. 3.
 0. 36. 202. 406. 581. 701. 764. 758. 692. 569. 391. 191. 33. 0.
 0. 9. 128. 319. 495. 620. 685. 680. 613. 490. 315. 125. 10. 0.
 0. 3. 85. 259. 425. 543. 605. 605. 538. 418. 255. 86. 3. 0.
 AVE AME TEMP. IN JAN,FEB,MAR,APR,MAY,JUN,JUL,AUG,SEP,OCT,NOV,DEC
 10.9 10.4 10.0 9.6 9.2 8.9 8.6 8.7 11.0 13.8 16.3 17.0 17.8 19.6
 15.7 15.6 15.1 17.2 15.5 14.1 13.2 12.6 11.7 11.3
 14.6 14.1 13.5 12.0 12.7 12.3 12.0 12.4 15.2 17.9 19.2 21.7 23.0
 23.6 23.7 23.8 23.4 22.0 20.0 18.6 17.5 16.8 16.0 15.4
 12.5 18.9 18.4 17.7 13.3 16.8 16.6 16.0 21.1 23.6 25.7 27.1 28.0
 28.6 28.9 28.7 28.4 27.2 25.3 23.7 22.6 21.8 21.0 19.3
 25.6 24.6 24.2 23.5 22.7 22.6 22.5 24.7 28.1 30.5 32.2 33.5 34.3
 34.8 35.1 34.9 34.7 33.7 31.9 30.2 29.0 28.0 27.4 26.5
 29.1 28.4 27.8 27.2 26.7 26.3 27.1 29.3 31.8 34.1 35.7 36.9 37.7
 38.3 38.5 38.7 38.8 37.5 35.9 34.1 32.6 31.5 30.7 29.0
 31.7 31.2 30.7 30.4 30.0 29.6 30.0 31.4 33.6 34.7 35.9 36.8 37.7
 38.3 38.5 38.4 38.2 37.7 36.7 35.4 34.3 33.6 32.7 32.3
 29.7 29.4 29.1 28.8 28.6 28.4 28.6 29.3 30.5 31.2 32.0 32.8 33.3
 33.6 33.7 33.7 33.4 33.0 32.4 31.5 31.0 30.5 30.1 29.7
 27.9 27.7 27.5 27.2 27.1 27.2 28.0 28.6 29.5 30.3 30.9 31.3
 31.5 31.6 31.5 31.4 31.0 30.3 29.6 29.1 28.8 28.4 28.1
 26.7 26.4 26.1 25.9 25.7 25.5 25.6 26.5 28.1 29.2 30.3 31.1 31.6
 31.9 32.0 31.8 31.5 30.7 29.5 28.7 28.2 27.7 27.3 26.9
 22.6 22.7 21.8 21.5 21.1 20.8 20.8 22.3 25.2 27.0 28.5 29.8 30.4
 31.2 31.3 31.1 30.6 29.0 27.2 25.9 25.0 24.4 23.5 23.0
 16.5 16.0 15.5 15.1 14.8 14.5 14.3 15.3 18.9 21.6 23.7 25.2 25.9
 26.2 26.4 26.0 25.2 22.9 20.9 19.6 18.7 18.0 17.3 16.8
 11.5 11.0 10.6 10.3 10.1 9.7 9.5 9.8 12.3 14.9 17.3 19.0 20.1
 20.7 20.9 20.7 19.7 17.2 15.9 14.7 13.9 13.2 12.5 11.9
 60 81 83 85 83 86 87 87 79 67 57 49 44 41 38 36 40 47 57 65 69 72
 75 77 AVE. RH IN JAN.
 65 68 70 72 73 75 76 73 63 53 44 38 34 31 29 28 29 33 41 48 53 57
 54 62 AVE. RH IN FEB.
 56 59 61 64 66 66 69 66 64 46 38 34 30 27 26 25 25 28 33 39 44 47
 50 53 AVE. RH IN MARCH
 40 42 45 47 48 51 52 47 39 34 30 26 23 21 19 19 19 20 23 26 30 32
 35 37 AVE. RH IN APRIL

37 39 41 42 44 46 46 43 37 34 30 26 24 22 20 20 19 19 22 25 29 32
 33 36 AVE. RH IN MAY
 47 49 51 53 54 56 56 54 48 45 41 37 34 32 31 30 30 30 32 33 39 41
 44 46 AVE. RH IN JUNE
 76 78 79 80 81 82 81 79 73 68 64 61 59 58 56 57 57 58 61 66 69 72
 74 75 AVE. RH IN JULY
 87 88 89 87 90 90 88 80 77 73 70 68 67 66 67 67 69 79 78 81 83
 85 86 AVE. RH IN AUG
 83 44 85 85 86 86 87 84 74 68 63 58 56 54 53 54 55 57 66 71 75 78
 80 81 AVE. RH IN SEPT.
 73 75 77 78 79 80 80 76 63 54 48 42 38 36 34 34 37 43 51 58 63 66
 69 70 AVE. RH IN OCT.
 70 73 75 76 78 79 80 78 64 53 43 39 35 32 31 31 34 42 50 56 60 63
 66 67 AVE. RH IN NOV.
 79 80 81 83 84 85 86 86 76 65 56 49 43 40 38 38 41 50 60 66 70 73
 75 77 AVE. RH IN DEC
 0. LOAD